Applied Clay Science 235 (2023) 106879

Contents lists available at ScienceDirect

Applied Clay Science

journal homepage: www.elsevier.com/locate/clay

Research Paper

Use of response surface methodology to optimize triclosan adsorption on alumina pillared clays in a fixed-bed column for applications in solid-phase extraction

Yaneth Cardona, Sophia A. Korili, Antonio Gil *

INAMAT˜2-Departamento de Ciencias, Edificio de los Acebos, Universidad Pública de Navarra, Campus de Arrosadía, Pamplona 31006, Spain

ARTICLE INFO

Keywords:
Adsorption
Emerging pollutants
Solid-phase extraction
Response surface methodology
Pillared clays

ABSTRACT

Fixed-bed column studies are generally conducted to consider possible applications in water-purification processes. In this work, three synthetic alumina pillared interlayered clays (Al-PILC) were analyzed in fixed-bed column studies for use as sorbents for solid-phase extraction (SPE) for the first time. Adsorption processes were studied for triclosan (TCS), which is an emerging pollutant (EP) that has been shown to have several health effects. Breakthrough curves were investigated by varying process parameters such as bed height (0.25–0.75 cm), inlet TCS concentration (20–60 mg/cm^3), and flow rate (0.5–3 cm^3/min). Bohart-Adams, Bed Depth Service Time (BDST), and Thomas models were satisfactory applied to the results obtained for fixed-bed columns. The adsorption of TCS was successfully optimized for use in SPE for the three adsorbents studied using response surface methodology with a Box–Behnken design (RSM-BBD). The models developed were adequate for the experimental data (95% significance level), with high regression parameters (98.9–99.1). The optimum values for TCS adsorption on the fixed-bed column were 378.04, 367.78, and 378.93 mg (amount of adsorbent packed into the column), 0.5 cm^3/min (flow rate), 4.24, 3.96, and 3.85 (pH), and 2.56, 1.93, and 1.13 mg/dm^3 (inlet TCS concentration) for Al-PILC$_{AE}$, Al-PILC$_{BE}$, and Al-PILC$_{CM}$, respectively. From these results synthetic Al-PILC are effective and promising sorbents that can be used for analytical purposes in SPE, and that RSM-BDD is an effective and reliable tool for evaluating and optimizing the adsorption conditions for emerging contaminants in a fixed-bed column system.

1. Introduction

Amongst the organic pollutants of greatest concern are the Emerging Pollutants (EP). EP includes those chemicals that were not considered as pollutants in the past, but that currently and because of their abuse and their released into the environment have grown in concentration to the point of be consider harmful today (Palencia et al., 2021). One example of EP is the Triclosan (TCS; 5-chloro-2-(2,4-dichlorophenoxy)phenol) that belongs to the chlorophenol (CP) family. TCS is a synthetic preservative, antibacterial and antifungal agent used in several domestic, consumer, household, and personal care products such as antibacterial soaps, deodorants and toothpastes as well as cosmetics and various types of sanitization (Mezcua et al., 2004; Sanchez-Prado et al., 2006; Tohidi and Cai, 2017; Magro et al., 2020; Wang et al., 2021; Tenkov et al., 2022). TCS has been found in the aquatic environment (Tenkov et al., 2022) and it has been shown to be relate to the mitochondrial dysfunction and has several health effects, such as endocrine disruption, estrogenic effects, and stimulation of carcinogenesis (Mezcua et al., 2004; Sanchez-Prado et al., 2006; Tohidi and Cai, 2017; Magro et al., 2020; Wang et al., 2021; Tenkov et al., 2022). The use of TCS together with other disinfectants has increased in the last years, especially due to the COVID−19 pandemic (Tenkov et al., 2022). Due to its dangerous effects for the living organisms and its continued-increased concentration in the environment, its removal from water sources using various processes—including adsorption, biodegradation, advanced oxidation, and combined methods, amongst others—has been studied (Wang and Liang, 2021).

The presence of pollutants in water also poses a challenge for laboratory techniques, especially as regards the determination of EP such as triclosan and drug residues, as they tend to be present in water sources at only low concentrations, thus requiring a concentration step prior to their determination and quantification in many cases. For this reason,

* Corresponding author.
E-mail address: andoni@unavarra.es (A. Gil).

https://doi.org/10.1016/j.clay.2023.106879
Received 1 November 2022; Received in revised form 7 February 2023; Accepted 21 February 2023
Available online 28 February 2023

new highly sensitive and selective analytical methods are increasingly necessary, along with efficient sample preparation, which removes interference components and concentrates target analytes prior to instrumental analysis and quantification, thus improving both method sensitivity and selectivity (Paíga and Delerue-Matos, 2013; Fu et al., 2022). Sample preparation is considered an essential step in chemical analysis, and in the last 20 years or so the development of "green sample preparation" such as Solid-Phase Extraction (SPE) which uses small amounts of solvent generating little waste has attracted considerable attention (Aly and Górecki, 2020; López-Lorente et al., 2022). This is due to the fact that the sample preparation step is considered to be potentially the most polluting step in analysis and green techniques reduce or eliminate this problem in accordance with the principles of green chemistry, including the limited energy, consumables, miniaturization, and quantity of solvents used (Dubé and Salehpour, 2014; López-Lorente et al., 2022; Raccary et al., 2022).

To achieve the accurate and reliable quantification of pollutants in samples, selection of the appropriate sample preparation technique is essential (Paíga and Delerue-Matos, 2013). In this regard, SPE has been used as a sample preparation methodology for a wide range of pollutants in matrices of environmental interest, especially water, due to its numerous advantages, including simplicity, flexibility, the possibility of using several sorbents, and the minimal use of solvent (1 to 5 cm^3), amongst others, thus allowing excellent recovery of the analytes (Poole, 2003; Paíga and Delerue-Matos, 2013; Maranata et al., 2021; Fu et al., 2022; Raccary et al., 2022). During SPE, the analytes are transferred from the mobile phase to the solid phase, where they are retained during the sampling process and then eluted and recovered using a liquid or a fluid (Poole, 2003). SPE has been used as a powerful tool for isolation (sample clean-up), concentration (trace enrichment), and medium exchange (transfer of the solute from the sample matrix to a solvent) of trace analytes in several sample matrices, generally coupled to both Liquid Chromatography (LC) and Gas Chromatography (GC) (Poole, 2003; Paíga and Delerue-Matos, 2013). This sampling technique is widely used in many fields of chemistry, such as pharmaceutical, food, environmental, industrial, and clinical (Poole, 2003).

Given the extensive use of SPE, several sorbents have been developed and proposed to facilitate the isolation and concentration processes for several analytes in various samples, thus extending the scope of SPE methods (Poole, 2003). The sorbents used for SPE can be divided into three groups: inorganic oxides (alumina, silica gel, and diatomaceous earth, amongst others), low-specificity sorbents (chemically bonded sorbents such as silicas, carbon, and porous polymers, amongst others), and class-specific and compound-specific sorbents (such as molecular imprinted polymers, amongst others) (Poole, 2003). In the first two groups, the analytes are retained by way of non-specific interactions (Dahane et al., 2015; Fu et al., 2022), whereas in the third group selective sorbents based on bioaffinity, ion exchange, etc., retain the analytes in a selective manner (Poole, 2003).

Several adsorbents can be used as stationary phases in SPE. The adsorption efficiency depends, amongst other factors, on the nature of the adsorbent used in the process (Allouss et al., 2019); thus making that several studies have focused on studying diverse natural and synthetic materials as adsorbents of organic compounds (Cardona et al., 2022), expanding the probable spectrum of solids that can be used. On the other hand, the modification of the known adsorbents to develop new adsorbents with enhanced properties, including high adsorption capacity and fast adsorption rate, also have been studied (Zheng and Wang, 2010). Clays and pillared interlayered clays (PILC) are perhaps the solids most widely studied as adsorbents for a wide range of organic pollutants, including EP. Although alumina pillared interlayered clays (Al-PILC) are generally obtained using an aluminum salt, some researchers have recently shown that they can be synthesized using other aluminum sources, such as saline slags, which are a hazardous waste obtained from the secondary aluminum production process. The resulting Al-PILC showed high adsorption capacities for three EP, including TCS (Cardona et al., 2021). This fact supports the effective new low-cost adsorbents for emerging pollutants that are needed, especially because they are derived from natural materials or wastes that are desired for both financial and technological reasons (Iqbal et al., 2016; Allouss et al., 2019).

However, most studies related to adsorbents have been conducted in either equilibrium or batch mode that cannot give accurate scale-up data (Maiti et al., 2008; Samarghandi et al., 2014). In contrast, experiments in fixed-bed systems with continuous flow help to obtain design models that are useful for this purpose (Maiti et al., 2008). Additionally, at the lab scale, the fixed bed column studies could allow the evaluation of the adsorbents for other purposes like for example, their use in routinary techniques as the preparation of samples such as SPE. The use of an adsorbent in the SPE cartridge allows us to study the adsorption process as a fixed-bed column, since optimization of the adsorption process in this case is equivalent to the SPE procedure. As the more selective the SPE extraction is, the more sensitive the method will be, careful optimization of the SPE-extraction parameters is necessary to reach the highest effectiveness in the extraction of the analyte (Maranata et al., 2021). However, many SPE methods are not optimized and little consideration has been given to the chemistry involved in this process (Hennion et al., 1998). The parameters to be optimized are: concentration of the analyte in the sample, pH of the solution, bed height, and flow rate of the solution through the stationary phase.

However, those operating variables interact in a nonlinear manner (Allouss et al., 2019). The classical approach used to optimize those operating variables has been one-factor-at-a-time designs (Paíga and Delerue-Matos, 2013; Allouss et al., 2019). This conventional method involves studying only one factor at a time, varying it during the experiment while keeping the other factors constant (Abou-Taleb and Galal, 2018; Ani et al., 2019). This method does not study the interactions between the factors and requires a large number of individual experiments, thus making it a time-consuming and reagent-intensive method (Paíga and Delerue-Matos, 2013; Abou-Taleb and Galal, 2018; Allouss et al., 2019; Ani et al., 2019). As these interactions are nonlinear (Allouss et al., 2019), and given the limitations of the classical methodology, researchers have tried to find other options to optimize the adsorption process that allow the interactions between the operating factors to be studied and yield better results with fewer experimental runs.

The use of a statistical approach to optimize a process is a remarkable and powerful option. Such strategies are known as statistical experimental design (SED) and their use has several advantages, including the fact that they allow the interactions between the factors involved in the process to be evaluated. This not only shows the effect of each factor on the response, but also determines how this effect varies with a change in the other factors involved (Ani et al., 2019). SED overcomes the limitations of classical methodology by optimizing all parameters collectively in a lower number of experiments (Abou-Taleb and Galal, 2018; Ani et al., 2019). Indeed, this less time-consuming strategy has shown better results than the traditional method (Abou-Taleb and Galal, 2018).

Amongst the SED, response surface methodology (RSM) has been successfully used by researchers for the effective optimization of the adsorption process in batch systems (Zheng and Wang, 2010; Iqbal et al., 2016; Mourabet et al., 2017; Allouss et al., 2019). RSM is a collection of statistical techniques based on the multivariate non-linear model (Zheng and Wang, 2010; Ani et al., 2019) that has been shown to be a useful tool for reducing both the time and costs of the experimental runs required (Allouss et al., 2019). Its main goal is to find the optimum working conditions in a short time using a limited number of experimental runs (Allouss et al., 2019). The first step in RSM is to design experiments that provide reliable measurements of the response to be evaluated. Then, using these results, a mathematical model that gives the best fit to the experimental data is developed, and finally, the optimal values of the independent variables in the process are determined. These optimum values are those that together give the best result, in other words the

maximum or minimum response of the response evaluated (Zheng and Wang, 2010). In summary, RSM is a powerful mathematical tool for designing statistical modeling (Zheng and Wang, 2010) which, in addition to designing experiments and building the models, searches for the optimum experimental conditions by studying the effect of the parameters involved when changing them simultaneously (Allouss et al., 2019; Ani et al., 2019), thus implying a more efficient use of resources (Ani et al., 2019).

Fixed-bed column studies are generally conducted to consider possible applications in water-purification processes. However, as mentioned above, techniques such as SPE are widely used in the laboratory, therefore the study of new adsorbents that may prove useful for SPE is relevant, with this interest increasing recently due to the number of EP in water that need to be pre-concentrated prior to quantification. In this work, three Al-PILC were studied as adsorbents for TCS in a fixed-bed column using SPE cartridges as the columns. The adsorption of TCS was optimized for these three Al-PILC using a response surface methodology (RSM) with a Box–Behnken design (BBD) in order to use them as SPE sorbents. Two of the Al-PILC were synthesized from a hazardous waste known as saline slag, and all three Al-PILCs had exhibited high TCS adsorption capacities in a batch system in a previous study (Cardona et al., 2021).

2. Experimental procedure

2.1. Materials and reagents

Hydrochloric acid (37%, PanReac AppliChem) and sodium hydroxide (PanReac AppliChem) were used to vary the pH. Triclosan (TCS; 5-chloro-2-(2,4-dichlorophenoxy)phenol, $C_{12}H_7Cl_3O_2$, Alfa Aesar) was used as an aqueous solution in ultrapure water (Milli-Q apparatus - Millipore) and ethanol (PanReac AppliChem) to enhance its solubility. A Visiprep SPE Vacuum Manifold (SUPELCO) equipped with a vacuum pump (VidaXL) was used in all experiments.

The three adsorbents considered as stationary phases in this study are three Al-PILCs synthesized from various aluminum sources. One of the PILC (Al-$PILC_{CM}$) was synthesized using an aluminum salt ($AlCl_3{\cdot}6H_2O$) following the conventional hydrolysis reaction (OH^-/Al^{3+}). The other two Al-PILC were obtained using the aluminum extracted from saline slag waste using alkaline (Al-$PILC_{BE}$) and acidic (Al-$PILC_{AE}$) extraction techniques as synthetic precursors. The synthesis and complete characterization of these latter two Al-PILC are described in detail in a previous study (Cardona et al., 2021). In summary, the aluminum was extracted from the saline slag using hydrochloric acid (acidic extract) or sodium hydroxide (alkaline extract). Those extracts were used as precursors to prepare the intercalation solutions via titration and to synthesize Al-$PILC_{AE}$ and Al-$PILC_{BE}$ respectively. Several parameters were evaluated during the preparation of the intercalation solutions such as the $[OH^-]/[Al^{3+}]$ molar ratio (0.5–2.5), Al/clay (mmol/g) ratio (2−20), clay/volume solution (g/dm^3) ratio (2−10), and temperature (room temperature, 60 and 90 °C) as titration and aging temperatures. For all the experiments, the titration and aging time used was 1 h. For the intercalation process, the clay used was Montmorillonite – Mt. supplied by Tsukinuno – The Clay Science Society of Japan). Mt. was mixed with the respective intercalant solution under constant stirring (22 h at room temperature) and then it was separated by centrifugation (Hettich ROTANTA 460 S), washing several times the solid with distilled water. Then, the intercalated clay was dried (100 °C for 8 h) and calcined (500 °C for 4 h, 1 °C/min - Nabertherm L5/S27) obtaining the pillared clay. The present work uses the three Al-PILC obtained at those synthesis conditions which resulted in the highest textural properties, respectively. Fig. S1 shows the XRD patterns and N_2 adsorption-desorption isotherms of the raw Mt. used in the synthesis and the three Al-PILC used in this work. Fig. S2 and S3 show the SEM and TEM micrographs of them and Table S1 gives the values for their basal spacing (d_{001}), specific surface area (S_{BET}), total pore volume (V_{Total}), and average pore diameter (dp).

2.2. SPE procedure

A known quantity (mg) of the respective adsorbent was packed into the column, which was a 3-cm^3 empty polypropylene SPE cartridge (Supelco - internal diameter 1.4 cm, length 6.0 cm), equipped with Polyethylene (PE) Frits (20 μm porosity). A TCS aqueous solution of known concentration (mg/dm^3) was prepared using ultrapure water (Milli-Q apparatus - Millipore) and ethanol (PanReac AppliChem) to enhance their solubility. The pH of the solution was adjusted at the corresponding pH value and then it was passed continuously through the respective Al-PILC bed at a known and constant flow rate (cm^3/min). The Al-PILC packed into the cartridges was dried under vacuum for 10 min and elution was performed using 2 cm^3 of a 50% *v*/v solution of ethanol. All experiments were conducted at room temperature using a Visiprep™-SPE Vacuum Manifold (SUPELCO).

Before quantifying the TCS in each aliquot collected, the sample was filtered (0.45 μmol, Durapore). The TCS concentration was determined at 279.4 nm, which is the maximum absorption wavelength for this pollutant, using a spectrometer (Jasco V-730 UV–Vis). The percentages of TCS adsorbed and eluted were determined using the following equations:

$$\%TCS\ adsorbed = \left[\frac{C_i - C_f}{C_i}\right] * 100 \quad (1)$$

where C_i and C_f are the TCS concentration (mg/dm^3) at the beginning (inlet concentration) and end of the experiment (outlet concentration), respectively.

$$\%TCS\ eluted\ (\%) = \frac{m_e}{m_{ad}} * 100 \quad (2)$$

where m_e, and m_{ad} are the mass of TCS eluted and adsorbed, respectively.

2.3. Analysis of column data and breakthrough curves

In the first stage of the continuous flow experiment, the adsorbent at the top of the column saturates, thus resulting in the maximum possible removal in this adsorption zone. Subsequently, the adsorption zone moves down through the column as the experiment proceeds, until it reaches the exit of the bed in the column. At this point, the concentration of the respective adsorbate in the effluent equals the inlet concentration (Omidvar Borna et al., 2016). Study of the adsorption in a fixed-bed column system is relevant to predicting the column breakthrough (Samarghandi et al., 2014). Continuous flow experiments were therefore carried out to evaluate the column performance for TCS adsorption by the Al-PILC.

A plot of the ratios of both concentrations (effluent and inlet (C_t/C_o)) versus elapsed time (*t*) or respective effluent volumes (*V*) used is known as the breakthrough curve (Omidvar Borna et al., 2016). The breakthrough curve is vital for understanding the performance of the packed bed in the adsorption process in a fixed-bed system. Both the shape and times of appearance of the breakthrough curve are relevant as regards defining both the operation and the dynamic response of any adsorption column (Maiti et al., 2008; Omidvar Borna et al., 2016). In studies related to the adsorption of an analyte on fixed-bed columns, predicting information about the bed used—such as how long it will last before it needs to be regenerated and how much effluent it can treat—is relevant; this is a key objective in the design of adsorption columns (Maiti et al., 2008). To study the breakthrough curves, the column was run by varying the flow rate (0.5, 1.0, and 3 cm^3/min), bed depth (0.25, 0.5, and 0.75 cm, equivalent to 100, 200, and 300 mg of adsorbent, respectively), and initial concentration (20, 40, and 60 mg/dm^3) individually while keeping the other parameters (0.5 cm^3/min, 0.75 cm or

20 mg/dm^3) constant. The pH used was 4 in light of the preliminary results (Cardona et al., 2021). Adsorption was carried out in the SPE system as explained previously, by collecting aliquots at regular time intervals from the outlet of the column until the effluent TCS concentration (C_t) approached the initial concentration (C_0), and the exhaustion time (t_e) was noted ($C_t/C_o \geq 0.9$) (Vijayaraghavan et al., 2004; Patel, 2020). The effluent volume (V_e), breakthrough capacity ($Q_{0.3}$), adsorption zone (Δt), and length of the mass transfer zone (Z_m) were calculated using Eqs. (3–6).

$$V_e = F^* t_T \tag{3}$$

$$Q_{0.3} = \frac{t_b\ (30\%)^* F^* C_o}{1000^* m} \tag{4}$$

$$\Delta t = t_e - t_b\ (30\%) \tag{5}$$

$$Z_m = Z\left(1 - \frac{t_b}{t_e}\right) \tag{6}$$

where V_e is the effluent volume (cm^3); F is the volumetric flow rate (cm^3/min); t_T is the total flow time (min); $Q_{0.3}$ is the breakthrough capacity ($mg_{TCS}/g_{adsorbent}$) at 30% or $Ct/C_o = 0.3$, t_b (30%) is the breakthrough time at 30% (min); C_o is the initial TCS concentration (mg/dm^3); m is the adsorbent mass (g); t_e is the exhaustion time; and Z is the bed depth (cm).

Eq. (7) was used to calculate the empty bed contact time (EBCT). The EBTC affects both the volume required to achieve breakthrough and the shape of the breakthrough curve (Samarghandi et al., 2014).

$$EBCT = \frac{V_c}{F} = \frac{Z}{U} \tag{7}$$

where V_c, F, Z, and U are the adsorption bed volume (cm^3), volumetric influent flow rate (cm^3/min), bed depth (cm), and linear flow rate (cm/min), respectively.

To analyze breakthrough profiles, several fixed-bed models based on film-pore and combined film-pore-solid diffusion theories have been proposed by different authors over the years (Walker and Weatherley, 1997). The results obtained in this work were analyzed using the Bohart and Adams, bed-depth service time (BDST), and Thomas models.

2.3.1. Bohart and Adams model

Bohart and Adams (1920) studied the adsorption of chlorine on charcoal and established the relationship between both bed depth (Z) and the time needed for breakthrough to occur (service time) (Bohart and Adams, 1920). The final model proposed is shown in Eq. (8). In this model, the adsorption rate is assumed to be proportional to both the concentration of the adsorbate and the residual capacity of the adsorbent toward the adsorbate (Maiti et al., 2008)

$$ln\left(\left(\frac{C_o}{C_t}\right) - 1\right) = N_o\ K_{AB}\ \frac{Z}{U} - K_{AB} C_o t \tag{8}$$

where C_0 and C_t are the concentration of adsorbate at the inlet and effluent, respectively, at any time (t), and N_o, K_{AB}, Z, and U are the adsorption capacity coefficient, the kinetic constant, the column height, and the linear velocity of the fluid, respectively. The adsorption capacity coefficient and kinetic constant are determined using a nonlinear regression (Maiti et al., 2008).

2.3.2. Bed-depth service time (BDST) model

The model proposed by Bohart and Adams in 1920 was linearized by Hutchins in 1973. The resulting simplified BDST design model is the most widely used (Walker and Weatherley, 1997; Samarghandi et al., 2014) and has been suggested by several authors to be the one that offers the simplest method and the fastest prediction of adsorbent performance (Walker and Weatherley, 1997). It is based on a surface chemical reaction rather than diffusion (Samarghandi et al., 2014).

In 1973, Hutchins proposed a simplified version (Eq. (9)) of this model, known as the Bed Depth Service Time (BDST) model (Hutchins, 1973), which allows the service time (t) for a specified bed depth (Z) to be determined. Both t and Z are correlated with the process parameters.

$$t = \frac{N_o}{C_o U} Z - \frac{1}{K_{AB} C_o} ln\left(\frac{C_o}{C_t} - 1\right) \tag{9}$$

Hutchins expressed the Bohart-Adams equation as a linear equation ($t = a\ Z + b$) relating the bed depth and time, with the slope (a) corresponding to Eq. (10) and the intercept (b) to Eq. (11) (Walker and Weatherley, 1997; Maiti et al., 2008).

$$a = \frac{N_o}{C_o U}, \tag{10}$$

$$b = -\frac{1}{K_{AB} C_o} ln\left(\frac{C_o}{C_t} - 1\right) \tag{11}$$

The adsorptive capacity (N_o) and rate constant (K_{AB}) can therefore be calculated from the slope and the intercept of a linear plot of t versus Z, respectively. Both the slope and intercept values obtained for one flow rate can be used to calculate the slope and intercept for other flow rates using the BDST model. In the case of the slope, the new slope can be calculated by multiplying the original one (a) by the ratio of the flow rates (original and new one). In this case, an adjustment of the intercept (b) is not necessary as the change in flow rate does not affect it significantly (Maiti et al., 2008). BDST has also been proposed for adjusting the data related to the inlet concentration (Maiti et al., 2008). Thus, for an inlet concentration C_1, the equation for a certain percentage saturation will be $t = a_1\ Z + b_1$. Eqs. (12 and 13) can be used to calculate both the slope (a_2) and intercept (b_2), respectively, for another inlet concentration (C_2). $C_{1'}$ and $C_{2'}$ in Eq. (13) correspond to both effluent concentrations.

$$a_2 = a_1\ \frac{C_1}{C_2} \tag{12}$$

$$b_2 = b_1\ \left(\frac{C_1}{C_2}\right)\ \frac{ln\left(\frac{C_2}{C_{2'}} - 1\right)}{ln\left(\frac{C_1}{C_{1'}} - 1\right)} \tag{13}$$

Finally, the use of $t = 0$ in Eq. (9) and solving for Z leads to Eq. (14):

$$Z_{min} = \frac{U}{K_{AB} N_o}\ ln\left(\frac{C_o}{C_t} - 1\right) \tag{14}$$

where the critical depth (Z_{min}) corresponds to the theoretical minimum column height needed to avoid penetration of the concentration in excess at zero time.

2.3.3. Thomas model

The Thomas model assumes that the adsorption process is limited by the mass transfer at the interface rather than by chemical interactions (Omidvar Borna et al., 2016). Thomas (1944) expressed adsorption on the column as:

$$\frac{C_t}{C_o} = \frac{1}{1 + exp\ \left(K_{Th} q_o \frac{m}{F} - K_{Th} C_o t\right)} \tag{15}$$

The linearized form of this model (Thomas, 1944) is shown in Eq. (16):

$$ln\left(\frac{C_o}{C_t} - 1\right) = \frac{K_{Th}^* q_o^* m}{F} - K_{th}^* C_o^* t \tag{16}$$

where K_{Th}, q_o, C_o, C_t, m, F, and t are the Thomas rate constant, the adsorption capacity, TCS initial concentration and TCS concentration at time t, the mass of adsorbent, flow rate, and flow time, respectively. The Thomas rate constant (K_{Th}) and adsorption capacity (q_o) are determined

from the slope and the intercept of a linear plot of $ln[(C_o/C_t) - 1]$ versus time (t).

2.4. Optimization of response surface methodology (RSM) with a Box–Behnken Design (BBD)

The three Al-PILC studied have been shown to be good adsorbents for TCS (Cardona et al., 2021). However, the conditions of the breakthrough curves are not necessarily those that lead to the highest TCS adsorption. Experimental design was used first to explore the conditions and then to find the optimum conditions for TCS adsorption by each of the three Al-PILC.

RSM is typically used to optimize the independent variables in a process to reach the maximum desired response. To that end, RSM uses a group of empirical techniques to establish the relationship between a cluster of independent experimental variables and their measured responses (Iqbal et al., 2016). As a result, RSM gives the following equation:

$$Y = \beta_0 + \sum \beta_i x_i + \sum \beta_{ii} {x_i}^2 + \sum \beta_{ij} x_i x_j \quad (17)$$

where Y is the predicted response; β_0, β_i, β_{ii}, and β_{ij} are regression coefficient constants for the model; and x_i and x_j $(i \neq j,\ i = 1 \rightarrow 4;\ j = 1 \rightarrow 4)$ correspond to the independent variables in the form of coded values (Zheng and Wang, 2010). This quadratic polynomial equation defines the behavior of the system and predicts the response as a function of the independent variables involved in the process, including their interactions. This information is relevant to understand the process studied (Zheng and Wang, 2010).

A multiple regression analysis method, based on the quadratic polynomial equation (Eq. 17), was used to estimate the coefficient of the model for the response.

An RSM based on a four-variable, three-level Box–Behnken Design (RSM-BBD) was used twice to evaluate and optimize the adsorption conditions in the fixed-bed column to achieve the maximum removal of TCS from the solution. The parameters evaluated in both cases were initial TCS concentration (20.0–50.0 and 1–30 mg/dm^3), sample flow rate (1.0–4.0 and 0.5–3.0 cm^3/min), pH (3.0–10.0 and 2.5–4.5), and adsorbent mass packed into the column (20–300 and 200–400 mg). SPE cartridges were used as the columns and a Visiprep™- SPE Vacuum Manifold (SUPELCO) was used in all experiments. All experiments were repeated twice, and the average values were used for data analysis. The ranges of the four variables studied in the first RSM-BBD were defined on the basis of the results obtained in breakthrough curve experiments in an attempt to study a wide range for every parameter and take into account the possible interactions between them. The ranges used in the second RSM-BBD were chosen on the basis of the results obtained in the first RSM-BBD. The three levels of the BBD factorial design used correspond to low, medium, and high, coded as −1, 0, and + 1, respectively. The ranges and levels studied in both RSMs are listed in Table 1. Both experiment design and RSM were carried out using Statgraphics (Centurion XIX). For statistical calculations, the four independent variables evaluated were designated as X_1 (pH), X_2 (adsorbent: amount of adsorbent packed into the column), X_3 (flux; sample flow rate), and X_4 (TCS concentration: inlet TCS concentration moving through the column), and were coded according to Eq. (18), where X_i, x_i, and x_0 are the values of an independent variable (dimensionless coded, real, and real at the center point, respectively); Δx_i is the step-change value (Zheng and Wang, 2010).

$$X_i = \frac{X_i - X_0}{\Delta X_i} \quad (18)$$

The runs resulting from the complete experimental design matrix were carried out in duplicate to optimize the level of the chosen variables mentioned previously. These runs were studied for each of the three adsorbents evaluated in this work (Al-PILC$_{AE}$, Al-PILC$_{BE}$, and Al-PILC$_{CM}$). In each case, average values were used for data analysis. The experiments were performed as discussed in the *"SPE Procedure"* section to obtain the percentage TCS adsorbed (Eq. (1)) in each case, which was the response evaluated.

The equations obtained were validated by statistical analysis of variance (ANOVA) in Statgraphics (Centurion XIX), which was also used for the regression analysis. ANOVA is the most reliable means of evaluating the quality of a fitted model (Iqbal et al., 2016; Shojaei et al., 2021). It examines the significance of the regression by comparing the share of variance for each factor with the variance caused by random errors in measurement (Mourabet et al., 2017; Shojaei et al., 2021). The *F-test* is used to make this comparison, with the resulting value being the ratio between the mean square of the model and the residual error (Mourabet et al., 2017). The *F-value* and *P-value* were used to verify the significance of each coefficient. Thus, the effect of a coefficient term is more significant as the smaller its value of P and the larger its value of F. 3D- and 2D-response surface plots were produced using the experimental data obtained to gain an overview of the effects of the independent variables. The models developed were used to predict the optimum conditions. Confirmatory experiments were conducted to evaluate the accuracy of this optimization.

Table 1
Ranges and levels for the four independent variables studied by RSM-BBD to optimize the adsorption of TCS on Al-PILC$_{AE}$, Al-PILC$_{CM}$, and Al-PILC$_{BE}$.

Variables		Range and level		
		−1	0	1
First Run				
X_1	pH	3	6.5	10
X_2	Adsorbent (mg)	20	160	300
X_3	Flux (cm^3/min)	1	2.5	4
X_4	TCS concentration (mg/dm^3)	20	35	50
Second Run				
X_1	pH	2.5	3.5	4.5
X_2	Adsorbent (mg)	200	300	400
X_3	Flux (cm^3/min)	0.5	1.75	3
X_4	TCS concentration (mg/dm^3)	1	15.5	30

3. Results and discussion

3.1. Analysis of column data and breakthrough curves

The values calculated for $Q_{0.3}$, V_e, Δt, and Z_m under the conditions studied are summarized in Table 2. The breakthrough curves obtained by varying the parameters bed depth (A–C), flow rate (D—F), and initial TCS concentration (G–I) individually are presented in Fig. 1. In the first stage, a fast uptake of TCS by the adsorbents was observed, followed by a rapid decrease until saturation was reached. This can be seen from the S-shaped curves, which show continued adsorption until the breakthrough point ($C_t/C_o = 0.3$) is rapidly reached, subsequently slowing to reach a value of 1. The change in the profile of the breakthrough curves due to the variations in the parameters mentioned is discussed in the subsequent sections.

3.1.1. Effect of bed height

To evaluate the effect of bed height, the column was run with three heights of 0.25, 0.5, and 0.75 cm, which correspond to 100, 200, and 300 mg of adsorbent, respectively, using an aqueous solution of TCS at 20 mg/dm^3 (pH 4) and a constant flow rate of 0.5 cm^3/min. The breakthrough curves obtained are shown in Figs. 1(A–C) for the three Al-PILCs. These curves show the change in the shape of the breakthrough curve due to the height of the adsorbent used. For the three Al-PILCs studied, the curves show that the use of a higher bed height results in a decrease in the slope of the respective curve while also increasing the adsorption capacity. This change in the slope of the breakthrough curves

Table 2
Breakthrough time, column sorption capacity, adsorption zone, and length of the mass transfer zone under several conditions using the Al-PILC as adsorbents.

Adsorbent	C_o (mg/dm^3)	F (cm^3/min)	m (mg)	Z (cm)	t_b (30%) (s)	V_e (cm^3)	$Q_{0.3}$ ($mg_{TCS}/g_{adsorbent}$)	Δt (min)	Z_m (cm)
	20	0.5	100	0.25	581	14	0.97	14.0	0.1
	20	0.5	200	0.50	1200	24	1.00	25.7	0.3
	20	0.5	300	0.75	2194	29	1.22	19.1	0.3
Al-PILC$_{AE}$	20	1.0	300	0.75	1041	40	1.16	18.3	0.4
	20	3.0	300	0.75	338	107	1.13	26.1	0.6
	40	0.5	300	0.75	450	16	0.50	20.2	0.5
	60	0.5	300	0.75	253	12	0.42	15.5	0.6
	20	0.5	100	0.25	268	10	0.45	11.2	0.2
	20	0.5	200	0.50	595	14	0.50	13.8	0.3
	20	0.5	300	0.75	1334	18	0.74	9.5	0.3
Al-PILC$_{CM}$	20	1.0	300	0.75	589	28	0.65	13.9	0.4
	20	3.0	300	0.75	187	35	0.62	8.6	0.5
	40	0.5	300	0.75	362	12	0.40	13.7	0.5
	60	0.5	300	0.75	175	8	0.29	8.8	0.6
	20	0.5	100	0.25	186	8	0.31	12.6	0.2
	20	0.5	200	0.50	395	12	0.33	13.1	0.3
	20	0.5	300	0.75	870	18	0.48	17.2	0.4
Al-PILC$_{BE}$	20	1.0	300	0.75	400	28	0.44	17.0	0.5
	20	3.0	300	0.75	130	35	0.43	9.5	0.6
	40	0.5	300	0.75	215	8	0.24	8.1	0.5
	60	0.5	300	0.75	120	6	0.20	5.7	0.6

C_o = the initial TCS concentration; F = the sample flow rate; m = the Al-PILC mass; Z = the bed height; t_b (30%) = the breakthrough time at 30%; V_e = the effluent volume; $Q_{0.3}$ = the breakthrough capacity at 30%; Δt = the adsorption zone; Z_m = the mass transfer zone.

is related to the enlargement of the mass transfer zone, as can be seen for the values calculated for Z_m in Table 2. Indeed, higher bed depths imply the use of higher amounts of adsorbent, which means more binding sites available for adsorption and higher breakthrough volumes (Vijayaraghavan et al., 2004; Maiti et al., 2008; Patel, 2020).

3.1.2. Effect of flow rate

The effect of flow rate was evaluated by comparing three flow rates (0.5, 1.0, and 3.0 cm^3/min) using a 20 mg/dm^3 solution of TCS at pH 4 and a bed depth of 0.75 cm (300 mg of adsorbent). The *EBCT* values calculated for 0.5, 1.0, and 3.0 cm^3/min were 9.6, 4.8, and 1.6 min, respectively. The breakthrough curves obtained (Figs. 1 D—F) show that the breakthrough curve was obtained faster for the highest flow rate used, thus resulting in a decrease in the volume treated to reach the breakthrough point (30%) (see Table 2), which means a decrease in the service time. The use of high flow rates results in a decrease in the contact time between both adsorbate and adsorbent, thus increasing the rate of mass transfer (Samarghandi et al., 2014; Patel, 2020). This corresponds to the amount of TCS adsorbed by the unit bed height or mass transfer zone, thus resulting in a faster saturation of the adsorbent. In contrast, a decrease in flow rate results in an increase in the contact time between adsorbate and adsorbent, thus facilitating penetration of the adsorbate into the pores of the adsorbent particle and resulting in a higher breakthrough capacity (Maiti et al., 2008). The volume required to reach the breakthrough point (30%) at the highest flow rate (3 cm^3/min) was around six- to seven-times lower than the volume required when using the lowest flow rate studied (0.5 cm^3/min). These results indicate that intraparticle diffusion plays an important role in the adsorption of TCS by the three PILCs in the fixed-bed column system at a low effluent flow rate.

3.1.3. Effect of initial TCS concentration

To investigate the effect of TCS concentration on the breakthrough curves, experiments were performed using inlet solutions of TCS at 20, 40, and 60 mg/dm^3 at pH 4. The breakthrough curves obtained using these solutions in a column with a bed depth of 0.75 (300 mg) and a constant flow rate of 0.5 cm^3/min are shown in Figs. 1 G–I. An increase in TCS concentration in the solution passing through the column resulted in a marked decrease in the volume treated to reach the breakthrough point (30%). These values changed from around 10–22 cm^3 at the lowest concentration tested (20 mg/dm^3) to approximately 2–3 cm^3 using the highest concentration tested (60 mg/dm^3). The shape of the breakthrough curve changed due to the increase in the concentration used, thus suggesting a possible saturation of the adsorbent, which may result in a decrease in the breakthrough time. The sharper breakthrough curve obtained at 60 mg/dm^3 compared with the curve obtained at 20 mg/dm^3 demonstrates that the change in the concentration used affects both saturation rate and breakthrough times. Thus, higher inlet concentrations of the adsorbate result in rapid saturation of the adsorbent in the bed, while lower concentrations require more time to achieve this due to the lower concentration gradient (Maiti et al., 2008; Patel, 2020).

3.1.4. Models used to analyze the breakthrough curves

The experimental data from the breakthrough curves obtained were fitted using the Bohart-Adams, bed-depth service time (BDST), and Thomas models. The parameters calculated using the BDST model at 20%, 30%, and 40% breakthrough are shown in Table S2, and the parameters calculated using the Thomas model at bed depths of 0.25, 0.50, and 0.75 cm are shown in Table S3. A comparison of the BDST and Thomas curves for the three Al-PILCs tested, using a bed depth of 0.75 cm and a TCS solution of 20 mg/dm^3 at a constant rate of 0.5 cm^3/min, can be found in Fig. 2. Both the BDST and Thomas curves show a similar profile for all three adsorbents. The equations calculated for the BDST model were t = 53.75 * Z – 4.79167 (Al-PILC$_{AE}$), t = 35.3956 * Z – 5.51113 (Al-PILC$_{CM}$), and Z = 22.80 * t – 3.3389 (AL-PILC$_{BE}$).

The parameters calculated using the Bohart-Adams, BDST, and Thomas models are provided in Table 3. As can be seen from this table, the experimental data are well fitted by the three models, thus indicating that all of them can be used to predict the adsorption performance for the adsorption of TCS in a fixed-bed column. The good fit achieved using the BDST model reflects the linear relationship between the service time of the column and bed depth (Lee et al., 2000). This fact is supported by the smaller values of K_{AB} (Table 3), since a longer bed is required to avoid breakthrough as its value decreases (Vijayaraghavan et al., 2004).

Although the three models used are highly valid for the adsorption of TCS by Al-PILC, the Thomas model gives the best fit, as can be seen from the higher R^2 values (0.981–0.988) and lower RSS values (1.80E-3–3.06E-3). This may be because the Thomas model assumes that the process data follow second-order kinetics and Langmuir isotherms (Omidvar Borna et al., 2016), which is in agreement with the results

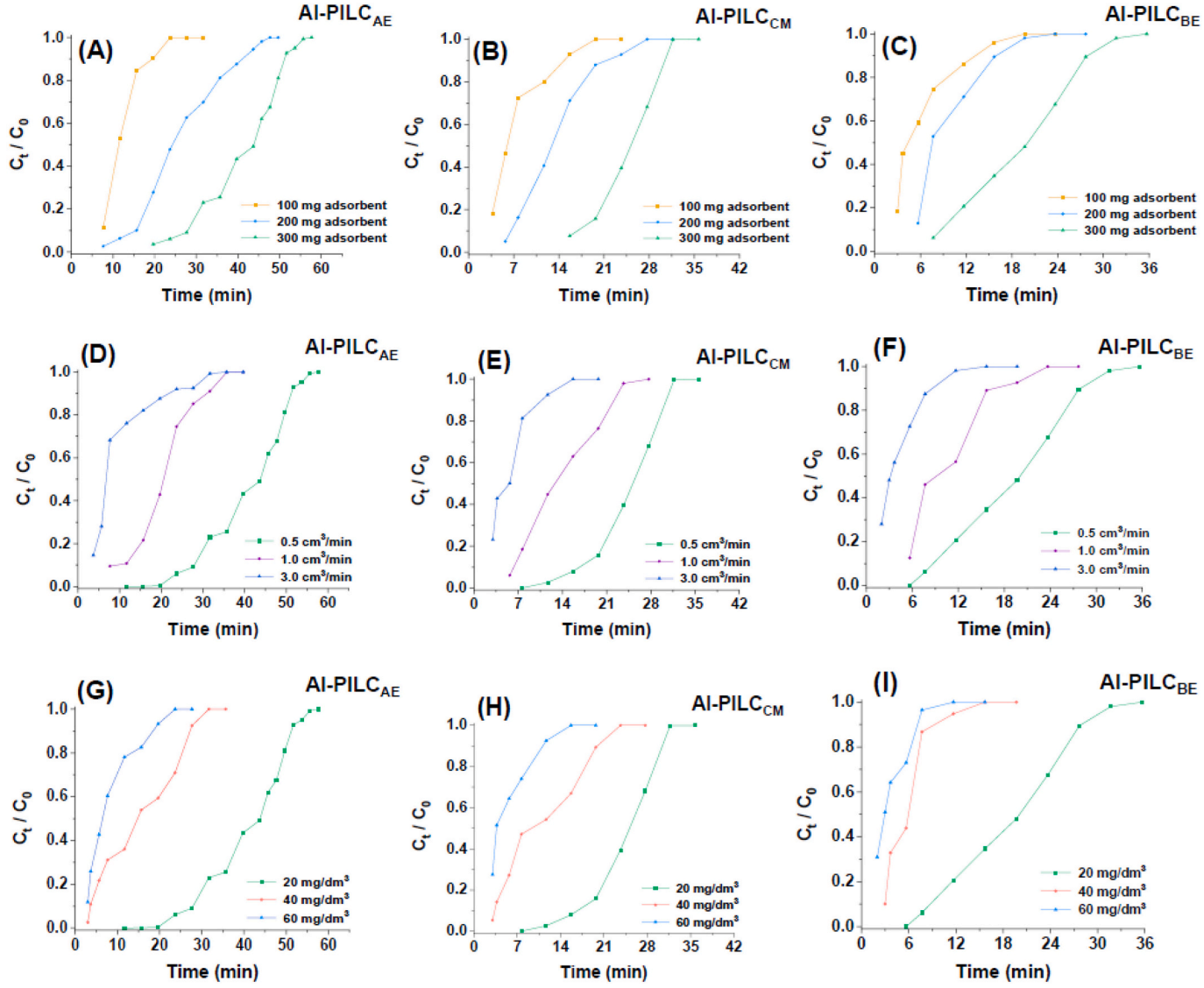

Fig. 1. Breakthrough curves obtained for TCS on an Al-PILC fixed-bed column using various bed depths (A, B, and C), flow rates (D, E, and F), and TCS concentrations (G, H, and I).

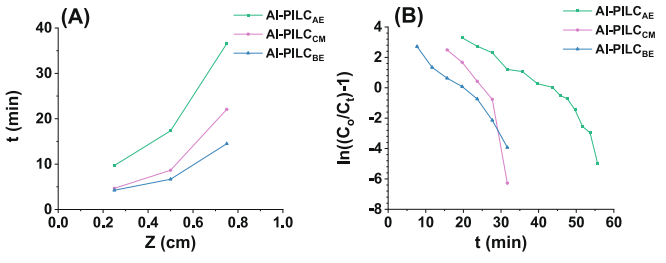

Fig. 2. (A) BDTS curves at 30% breakthrough and (B) Thomas curves for the three Al-PILCs for the removal of TCS with an inlet solution concentration of 20 mg/dm^3, at a constant flow rate of 0.5 cm^3/min, through a column with a bed depth of 0.75 cm (300 mg).

obtained in the batch experiments for the adsorption of TCS using these adsorbents (Cardona et al., 2021). The adsorption capacities of the column (0.75 cm) at the breakthrough point 0.5 ($Ct/C_o = 0.5$) calculated using the Thomas model were 1.37 (Al-PILC$_{AE}$), 0.83 (Al-PILC$_{AE}$), and 0.64 mg/g (Al-PILC$_{AE}$), which are very close to the experimental data obtained (1.46, 0.84, and 0.67 mg/g, respectively).

Table 3
BDST, Bohart-Adams, and Thomas model parameters for the removal of TCS by Al-PILC. Conditions: C$_o$: 20 mg/dm^3, Z: 0.75 cm, F: 0.5 cm^3/min.

Adsorption model	Parameters of the model	Al-PILC$_{AE}$	Al-PILC$_{CM}$	Al-PILC$_{BE}$
BDST	N_o (mg/g)	0.36	0.22	0.36
	K_{AB} (cm^3/mg·min)	8.60E-03	1.75E-02	8.77E-03
	R^2	0.98	0.98	0.98
	RSS	3.06E-03	3.05E-03	3.44E-03
Adam and Bohart model	N_o (mg/g)	2.76	4.64	5.99
	K_{AB} (1/mg·min)	8.77E-03	1.75E-02	1.06E-02
	R^2	0.98	0.98	0.97
	RSS	3.44E-03	2.97E-03	2.20E-03
Thomas	q_o (mg/g)	1.37	0.83	0.64
	K_{Th} (cm^3/mg·min)	8.60E-03	1.75E-02	1.06E-02
	R^2	0.98	0.990	0.990
	RSS	3.06E-03	2.79E-03	1.80E-03

3.1.5. Comparison between Al-PILC

The three adsorbents studied showed a similar behavior when each of the three parameters (bed height, flow rate, or concentration) were modified. The results obtained suggest that higher breakthrough volumes are obtained for a high bed depth, low inlet flow rate, and low inlet concentration for all three Al-PILC. Similarly, the results obtained upon varying the three parameters agree with those reported by other authors who have studied the adsorption of other pollutants, such as heavy metals (Vijayaraghavan et al., 2004; Goel et al., 2005; Omidvar Borna et al., 2016; Patel, 2020), arsenate (Maiti et al., 2008), and dyes (Samarghandi et al., 2014).

The highest values breakthrough capacities obtained at this point were achieved using 300 mg of adsorbent (0.75 cm bed depth), a flow rate of 0.5 cm^3/min, and 20 mg/dm^3 of TCS at pH 4 as the inlet concentration. A comparison of the breakthrough curves obtained for TCS adsorption by the three Al-PILC fixed-bed columns under these conditions is summarized in Fig. 3. As can be seen from that figure, and as already discussed, the breakthrough curve obtained under those conditions using the three Al-PILCs was not very steep compared with the breakthrough curves obtained under the other conditions tested, which means that exhaustion of the bed was not very fast compared with the others. Al-$PILC_{AE}$ had the highest column capacity, followed by Al-$PILC_{CM}$, and Al-$PILC_{BE}$. This difference is related to the differences between their morphologies and textural characteristics, such as their basal spacing (d_{001}) and specific surface area (S_{BET}; see Table S1).

3.2. Adsorption and response surface methodology (RSM)

3.2.1. Preliminary experiments

Since the breakthrough curves showed that the three Al-PILC exhibit similar behavior, Al-$PILC_{CM}$ was chosen for the preliminary experiments and then all of them were studied to find the optimum conditions for each. Taking into account the conditions, the EBCT calculated for each, and the intention to use them for SPE, 3 cm^3 were chosen as the solution volume to optimize the adsorption of TCS by the three Al-PILCs in the cartridges. To select the range for each of the four parameters to be optimized, an initial Box-Behnken design was developed using Al-$PILC_{CM}$ as adsorbent. The ranges tested in this preliminary experiment are shown in Tables 1 and S4. The response surface plots obtained showed that the highest amount of TCS was adsorbed under the conditions included in Fig. 4: at acidic pH (3–5), at low initial concentrations of the pollutant (20–30 mg/dm^3), using around 230–300 mg of adsorbent, and using a sample flow rate of 1–1.5 cm^3/min through the column. However, the highest adsorption was always at one extreme of the values tested. For this reason, the ranges of the four parameters to be optimized were stabilized, as shown in Table 1.

3.2.2. Optimization of adsorption parameters using Response Surface Methodology (RSM)

The adsorption response (%) obtained in the 27 experiments carried out for each of the three adsorbents tested is summarized in Table 4. The empirical relationship between the amount of TCS adsorbed (%) and the four variables tested in coded units, as well as their interactions, for the three adsorbents evaluated can be seen in Eqs. (19–21).

$$Y - Al - PILC_{AE} = 21.3593 + 5.0703 \times {}_1 + 0.3494 \times {}_2 + 14.9953 \times {}_3 - 0.4256 \times {}_4 - 0.2863 \times {}_1{}^2 - 0.0004X_1X_2 - 2.948X_1X_3 - 0.0926X_1X_4 - 0.0004 \times {}_2{}^2 - 0.0221X_2X_3 + 0.001X_2X_4 - 1.4224 \times {}_3{}^2 + 0.3771X_3X_4 - 0.0526 \times {}_4{}^2. \quad (19)$$

$$Y - Al - PILC_{BE} = 9.39772 + 11.7366 \times {}_1 + 0.2885 \times {}_2 + 13.7808 \times {}_3 - 0.3682 \times {}_4 - 1.2338 \times {}_1{}^2 + 0.0006X_1X_2 - 2.77X_1X_3 - 0.1803X_1X_4 - 0.0004 \times {}_2{}^2 - 0.0174X_2X_3 + 0.0015X_2X_4 - 1.44 \times {}_3{}^2 + 0.3375X_3X_4 - 0.0408 \times {}_4{}^2. \quad (20)$$

$$Y - Al - PILC_{CM} = 14.2304 + 9.7283 \times {}_1 + 0.3141 \times {}_2 + 14.2827 \times {}_3 - 0.4133 \times {}_4 - 1.0946 \times {}_1{}^2 + 0.0009X_1X_2 - 2.754X_1X_3 - 0.1309X_1X_4 - 0.0004 \times {}_2{}^2 - 0.0209X_2X_3 + 0.0010069X_2X_4 - 1.4645 \times {}_3{}^2 + 0.3761X_3X_4 - 0.0469 \times {}_4{}^2. \quad (21)$$

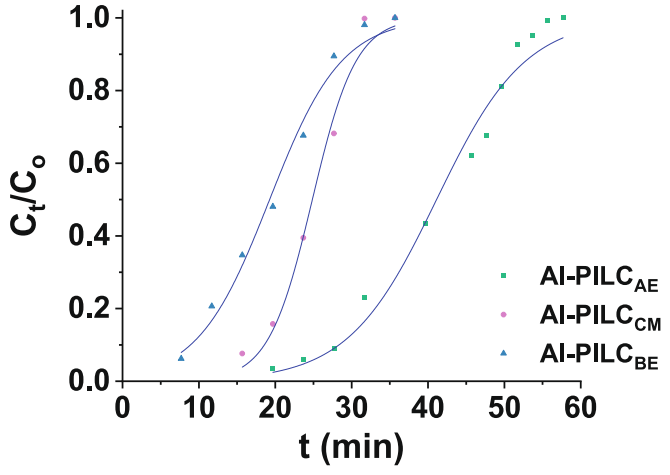

Fig. 3. Breakthrough curves obtained for TCS adsorption by the three Al-PILC fixed-bed columns using bed depths of 0.75 cm, and a 20 mg/dm^3 TCS solution at a constant flow rate of 0.5 cm^3/min. The blue line corresponds to the adjusted Thomas model. (For interpretation of the references to colour in this figure legend, the reader is referred to the web version of this article.)

where Y is the amount of TCS adsorbed (%) and X_1, X_2, X_3, and X_4 are the independent factors evaluated, namely pH, amount of adsorbent (mg), sample flow rate (cm^3/min), and initial TCS concentration (mg/dm^3), respectively. The sign before every independent factor or quadratic or double interaction term indicates the respective effect, with positive values indicating that an increase in their level leads to an increase in the response and negative values indicating that an increase in their levels leads to a decrease in the response (Demim et al., 2014; Allouss et al., 2019).

The ANOVA results for the preliminary experiment are shown in Table S5 and the ANOVA results for the quadratic Eqs. (19–21) are summarized in Tables 5–7. These values reveal the effects of all three interactions: first-order (X_1, X_2, X_3, X_4), pure quadratic (X_1^2, X_2^2, X_3^2, X_4^2), and two-way (X_1X_2, X_1X_3, X_1X_4, X_2X_3, X_2X_4, and X_3X_4). The results show that the three regressions for the TCS adsorption are statistically significant, with a $P\text{-}value < 0.05$ (95% significance) and an $F\text{-}value$ of 79.07–98.54. Analysis of the $F\text{-}value$ and the $P\text{-}value$ shows that the three regressions have eight (Al-$PILC_{AE}$) and nine (Al-$PILC_{BE}$ and Al-$PILC_{CM}$) significant model terms. The seven significant terms common to all three were X_1, X_2, X_4, X_1X_3, X_2^2, X_3X_4, and X_4^2. On the other hand, X_2X_3 and X_3^2 were significant common terms in a pair of different regressions, whereas X_2X_3 was a significant common term in the two regressions that

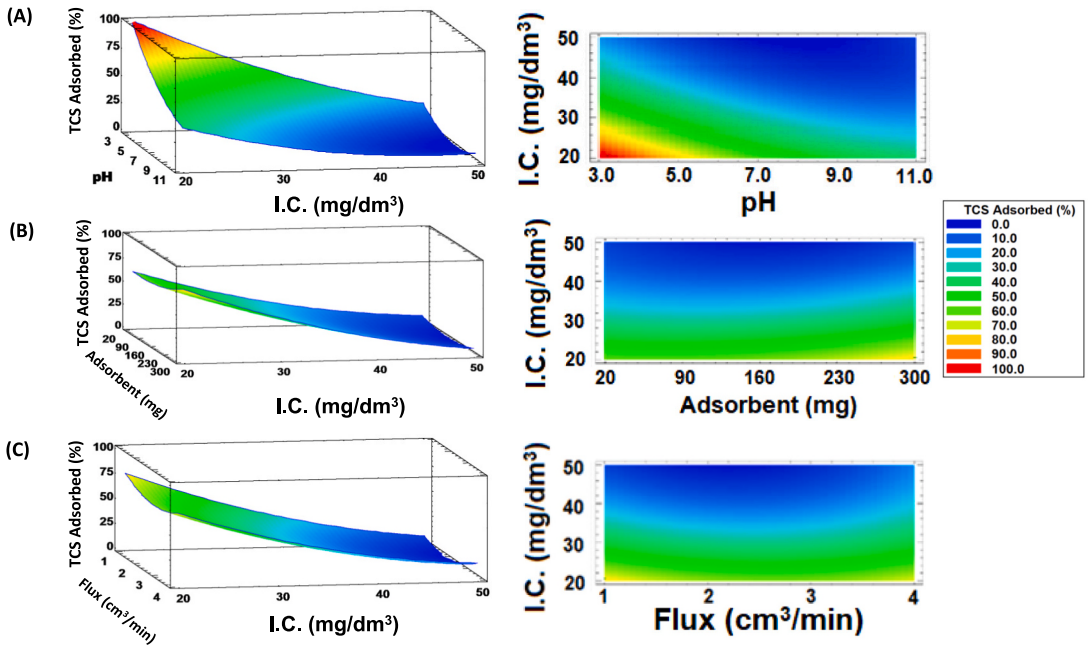

Fig. 4. 3D- and 2D-response surface plots of the effect of (A) pH and initial concentration with 160 mg of adsorbent and 2.5 cm^3/min flow rate, (B) amount of adsorbent and initial concentration at pH 6.5 and 2.5 cm^3/min flow rate, and (C) flow rate and initial concentration on TCS adsorption at pH 6.5 with 160 mg of adsorbent.

Table 4
BBD matrix in coded terms along with experimental values.

30	X_1	X_2	X_3	X_4	TCS adsorbed (%)		
					Al-PILC$_{AE}$	Al-PILC$_{BE}$	Al-PILC$_{CM}$
1	1	1	0	0	79.28	67.83	70.69
2	−1	0	−1	0	80.69	70.71	74.31
3	−1	0	0	1	52.99	49.71	49.82
4	0	0	0	0	81.93	73.28	76.53
5	0	−1	0	−1	85.22	74.76	79.41
6	0	0	1	−1	78.69	69.87	73.51
7	0	0	1	1	53.68	48.19	49.42
8	1	0	0	1	42.94	35.28	37.98
9	0	0	0	0	81.79	71.58	77.14
10	0	1	1	0	76.43	67.09	71.12
11	1	0	0	−1	90.72	80.00	84.66
12	−1	0	1	0	88.24	77.06	81.29
13	1	0	1	0	75.04	62.70	66.79
14	0	−1	0	1	42.06	36.34	38.35
15	0	0	−1	−1	97.31	85.83	90.85
16	0	−1	−1	0	68.40	60.56	63.57
17	1	−1	0	0	66.46	55.96	58.58
18	−1	1	0	0	88.00	77.30	81.87
19	0	1	0	1	54.66	51.99	50.43
20	0	0	−1	1	44.96	39.68	39.49
21	0	-1	1	0	70.63	62.10	65.53
22	1	0	-1	0	82.23	70.20	73.58
23	0	1	-1	0	85.23	74.26	79.60
24	-1	0	0	-1	95.40	83.97	88.91
25	0	0	0	0	84.14	72.58	75.47
26	-1	-1	0	0	75.03	65.66	70.13
27	0	1	0	-1	92.20	81.94	85.65

used Al-PILC$_{AE}$ and Al-PILC$_{CM}$ as adsorbents, and X_3^2 was a significant common term in those regressions that used Al-PILC$_{BE}$ and Al-PILC$_{CM}$ as adsorbents. Finally, X_1X_4 was only significant in the regression obtained using Al-PILC$_{BE}$ as adsorbent. These results are illustrated in the Pareto charts shown in Fig. 5, where the vertical line in the plots indicates the minimum statistically significant effect magnitude (95% confidence level). The good fit of the model can be verified by the determination coefficient R^2 (98.93, 99.0, and 99.1) and the lack of fit value ($P > 0.05$)

Table 5
ANOVA for the response surface quadratic model for TCS adsorption using Al-PILC$_{AE}$ as the adsorbent.

Source	Sum of squares	Degrees of freedom	Mean Squares	*F-Value*	*P-Value*
Model	6732.94	14	480.92	79.07	0.0126
X_1	159.00	1	159.00	26.14	0.0003
X_2	385.33	1	385.33	63.35	0.0000
X_3	21.63	1	21.63	3.56	0.0842
X_4	5135.67	1	5135.67	844.36	0.0000
X_1^2	0.44	1	0.44	0.07	0.7930
X_1X_2	0.01	1	0.01	0.00	0.9755
X_1X_3	54.32	1	54.32	8.93	0.0113
X_1X_4	7.21	1	7.21	1.19	0.2968
X_2^2	106.27	1	106.27	17.47	0.0013
X_2X_3	30.42	1	30.42	5.00	0.0452
X_2X_4	7.90	1	7.90	1.30	0.2773
X_3^2	26.34	1	26.34	4.33	0.0594
X_3X_4	186.87	1	186.87	30.72	0.0001
X_4^2	652.39	1	652.39	107.26	0.0000
Residual	72.9879	12	6.08		
Lack of fit	69.51	10	6.95	4.00	0.2164
Pure Error	3.48	2	1.74		
Corrected total	6805.93	26			

R^2 = 98.9; adjusted R^2 = 97.7; Pred R^2 = 94.0.

in all three cases, thus showing that the model appears to be adequate for the experimental data with 95% significance.

The R^2 values indicate a good fit between the predicted and experimental values in all three cases. This suggests that almost all the variations for the adsorption of TCS are explained by the independent variables tested in this work and their interactions, as expressed in the proposed mathematical model. As a result, the quadratic functions shown above can be used to successfully predict future responses for TCS adsorption on the three Al-PILC studied.

The model developed was used to predict the responses and then compare these values with the experimental values. The high degree of agreement between both experimental and predicted values (Y) over the range of independent variables selected can be seen in Fig. 6 A–C, which

Table 6
ANOVA for the response surface quadratic model for TCS adsorption using Al-PILC$_{BE}$ as the adsorbent.

Source	Sum of squares	Degrees of freedom	Mean Squares	*F-Value*	*P-Value*
Model	5141.22	14	367.23	89.19	0.0111
X_1	229.16	1	229.16	55.65	0.0000
X_2	352.41	1	352.41	85.58	0.0000
X_3	16.87	1	16.87	4.10	0.0658
X_4	3858.54	1	3858.54	937.03	0.0000
X_1^2	8.12	1	8.12	1.97	0.1856
X_1X_2	0.01	1	0.01	0.00	0.9557
X_1X_3	47.96	1	47.96	11.65	0.0051
X_1X_4	27.35	1	27.35	6.64	0.0242
X_2^2	77.32	1	77.32	18.78	0.0010
X_2X_3	18.97	1	18.97	4.61	0.0530
X_2X_4	17.94	1	17.94	4.36	0.0589
X_3^2	27.00	1	27.00	6.56	0.0250
X_3X_4	149.70	1	149.70	36.35	0.0001
X_4^2	393.19	1	393.19	95.49	0.0000
Residual	49.41	12	4.12		
Lack of fit	47.95	10	4.80	6.60	0.1386
Pure Error	1.46	2	0.73		
Corrected total	5190.63	26			

$R^2 = 99.0$; adjusted $R^2 = 97.9$ Pred $R^2 = 94.6$.

Table 7
ANOVA for the response surface quadratic model for TCS adsorption using Al-PILC$_{CM}$ as the adsorbent.

Source	Sum of squares	Degrees of freedom	Mean Squares	*F-Value*	*P-Value*
Model	6144.24	14	438.87	98.54	0.0101
X_1	243.45	1	243.45	54.66	0.0000
X_2	339.10	1	339.10	76.14	0.0000
X_3	15.73	1	15.73	3.53	0.0847
X_4	4700.52	1	4700.52	1055.41	0.0000
X_1^2	6.39	1	6.39	1.43	0.2541
X_1X_2	0.03	1	0.03	0.01	0.9316
X_1X_3	47.40	1	47.40	10.64	0.0068
X_1X_4	14.40	1	14.40	3.23	0.0973
X_2^2	87.68	1	87.68	19.69	0.0008
X_2X_3	27.25	1	27.25	6.12	0.0293
X_2X_4	8.53	1	8.53	1.91	0.1917
X_3^2	27.93	1	27.93	6.27	0.0277
X_3X_4	185.91	1	185.91	41.74	0.0000
X_4^2	518.59	1	518.59	116.44	0.0000
Residual	53.44	12	4.45		
Lack of fit	52.02	10	5.20	7.31	0.1262
Pure Error	1.43	2	0.71		
Corrected total	6197.68	26			

$R^2 = 99.1$; adjusted $R^2 = 98.1$; Pred $R^2 = 95.1$.

shows how the values are distributed close to the straight line. This relationship showed a reasonably high value for the coefficients of determination ($R^2 = 0.989–0.991$), thus indicating that the methodology used (RSM-BBD) can be successfully applied as an effective and reliable tool for evaluating and optimizing the adsorption conditions for TCS.

3.3. Effect of the parameters and their interactions

The 2D contour response surface plots obtained from the experimental data for each adsorbent are presented in Figs. 7–9. These diagrams are a function of two independent parameters, while keeping the other two parameters involved in the process constant. As such, these figures show the individual and cumulative effect of independent variables, and their combinations, on the adsorption efficiency. The contour plots show the dependency of adsorption efficiency on the initial concentration and the amount of adsorbent packed into the column (bed depth) (Figs. 7–9 A), the sample flow rate (Figs. 7–9 B), and pH (Figs. 7–9 C). Figs. 7–9 show that the adsorption efficiency increased in all three cases as the initial concentration of pollutant decreased (Figs. 7–9 C), the bed depth increased (Figs. 7–9 A), and the sample flow rate decreased (Figs. 7–9 B). The pH showed a less-marked behavior in the range tested (Figs. 7–9 C). However, higher adsorption of TCS was favored at acidic pH values, with this behavior being clearer in the case of Al-PILC$_{BE}$ (Fig. 8 C).

3.3.1. Effect of pH

pH is a critical parameter in adsorption processes since it strongly affects both sorbent and sorbate (Iqbal et al., 2016). Given the results obtained in the preliminary experiments (pH from 3 to 10), the pH was studied in the range of 2.5 to 4.5. The results of preliminary experiments (Tables S4, S5, and Fig. 4) showed that the pH is a critical parameter for the removal of TCS from solution. Indeed, pH is more relevant as it strongly affects both the surface charge of the solid phase used (the three adsorbents tested) and the degree of ionization and speciation of the adsorbate species (TCS). The highest adsorption capacity was achieved at acidic pH values, especially close to 4, which was the pH found to be suitable in the batch adsorption experiments carried out using these adsorbents previously (Cardona et al., 2021).

TCS is a weak acid with a pK_a value of 7.9 at 25 °C. The pH that favors the adsorption process is lower than this value, thus meaning that TCS molecules are almost undissociated And, therefore, that the dispersion interactions of TCS molecules predominate at this pH. The high content of these nonionized molecules in the mobile phase favors electrostatic attractions between them and the adsorption sites in the stationary phase rather than electrostatic repulsive forces (Tan et al., 2009). As mentioned previously, the surface characteristics of the adsorbents change upon modifying the pH of the solution (Iqbal et al., 2016). Thus, for example, their potential surface charge can vary due to the presence of OH^- or H^+ ions in the solution (Cardona et al., 2021). The point of zero charge (PZC) is the pH at which adsorbents have zero potential charge on their surface. The PZC for the adsorbents studied in this work was determined previously using the salt addition method (Cardona et al., 2021), giving values of 6.14 (Al-PILC$_{BE}$), 5.83 (Al-PILC$_{AE}$), and 5.91 (Al-PILC$_{CM}$). The pH that favors the adsorption process is lower than the pH$_{PZC}$ for the three adsorbents, thus meaning that the surfaces of all three adsorbents are positively charged due to the excess of H^+ ions in the solution, which protonate the surface functional groups. In the acid range the electrostatic attractions between the negative charges of the TCS molecules and the positive charges of the adsorbent surface increase, reaching a maximum at around pH 4. As the pH increases further, competition for the adsorption sites between the OH^- ions in the solution and the anionic ions of TCS appears at basic values, as do electrostatic repulsions between them (Toor and Jin, 2012), thus resulting in a decrease in TCS adsorption. This negative effect of increasing pH can be seen in Eqs. (19–21) and Fig. 5 for the three adsorbents studied.

The effect of pH with respect to the initial concentration of TCS (C), amount of adsorbent packed into the column (D), and flow rate (E) for all three Al-PILC studied is shown in Figs. 7, 8 and 9. Statistically, the pH effect (X_1) was significant for all Al-PILC, while its pure quadratic interaction (X_1^2) was not significant for any of them. The two-way interaction with flux (X_1X_3) was significant for all three Al-PILC and the two-way interaction with initial TCS concentration (X_1X_4) was significant only for Al-PILC$_{BE}$.

3.3.2. Effect of bed height

The amount of adsorbent packed into the column was studied in the range 200–400 mg (0.5–1.0 cm), generating response surface plots in combination with the initial TCS concentration (Figs. 7–9 A), pH (Figs. 7–9 D), and sample flow rate (Figs. 7–9 F) for the three adsorbents studied. The amount of adsorbent packed into the column affected TCS

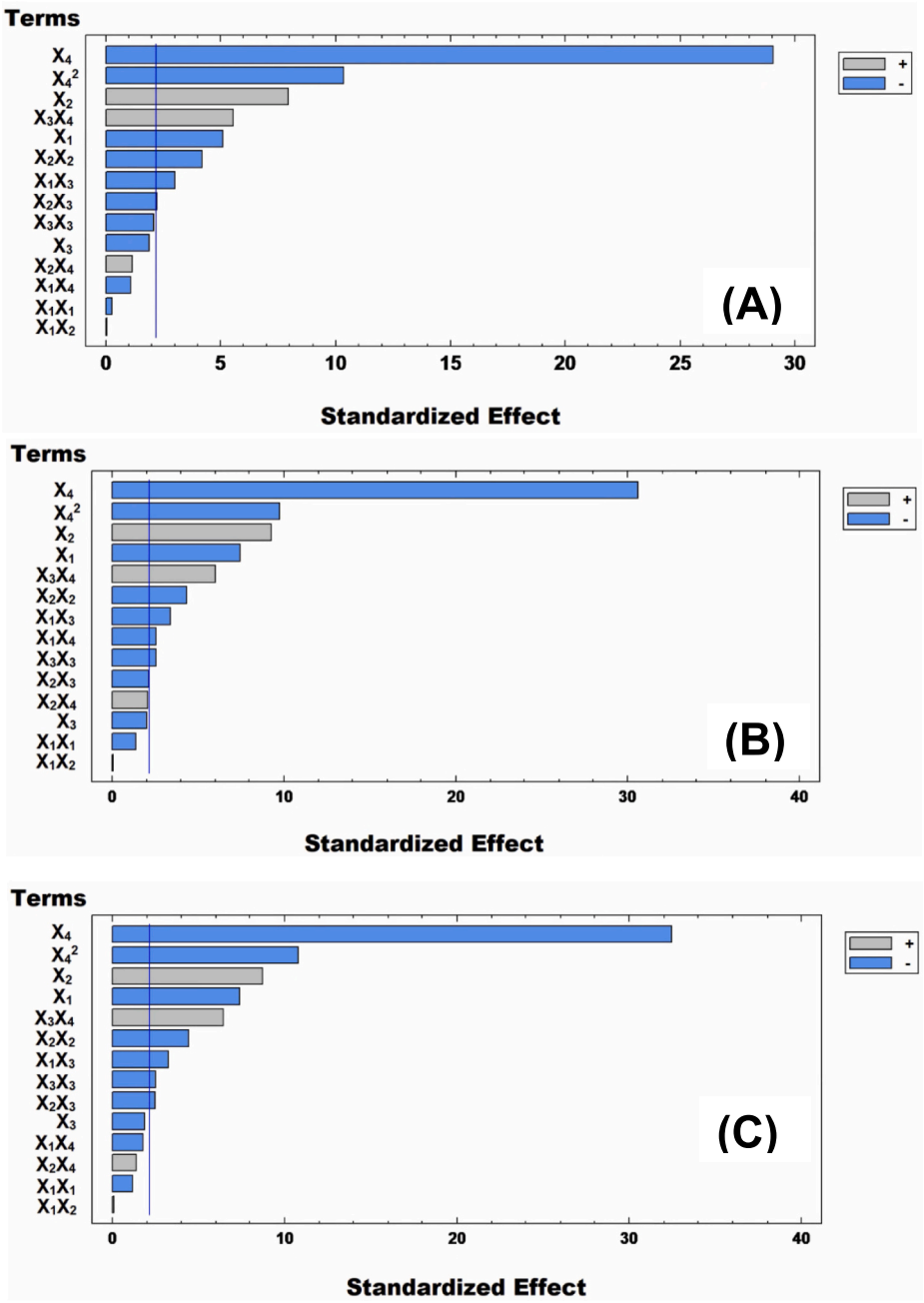

Fig. 5. Pareto Charts for (A) Al-PILC$_{AE}$, (B) Al-PILC$_{BE}$, and (C) Al-PILC$_{CM}$.

adsorption significantly in all three cases, with adsorption being higher at higher adsorbent amounts. This positive effect of adsorbent dose can be seen in Eqs. (19–21) and Fig. 5 for the three pillared clays studied and may be due to the fact that high amounts of adsorbent mean a higher surface area available for interaction with the adsorbate. However, the plots also show that the difference between the amounts of adsorbate adsorbed decreases as the amount of adsorbent increases. This suggests that the difference in the amount of TCS adsorbed starts to decrease statistically at some point, thus meaning that is not necessary to use the maximum adsorbent dose to absorb the maximum amount. Statistically, the adsorbent dose (X_2) and its pure quadratic interaction (X_2^2) were found to be significant for all three pillared clays studied. In contrast, the two-way interaction with the sample flow rate (X_2X_3) was significant for only two of the adsorbents (Al-PILC$_{AE}$ and Al-PILC$_{CM}$). However, it is the smallest effect amongst those considered as statistically significant.

3.3.3. *Effect of sample flow rate*

The sample flow rate (flux) was studied in the range 0.5–3 cm^3/min. Response surface plots of the sample flow rate in combination with the initial TCS concentration, pH, and length of the adsorbent bed used are shown in Figs. 7–9 B, E, and F, respectively. These plots showed that the percentage of TCS adsorbed decreases as the flow rate increases, especially above 1.5 cm^3/min. This change is more marked and easier to see for the combination flow rate and initial TCS concentration (Figs. 7–9 B). Lower flow rate values require more time to finish the experiment, thereby resulting in longer contact times between the mobile and stationary phases during the experiment.

Statistical analysis revealed that individual sample flow rate (X_3) did not have a significant effect on TCS adsorption for any of the three adsorbents, whereas it was close to the limit in the case of Al-PILC$_{BE}$ and its pure quadratic interaction (X_3^2) was significant for two of the three (Al-PILC$_{BE}$ and Al-PILC$_{CM}$). The interaction of sample flow rate with both pH

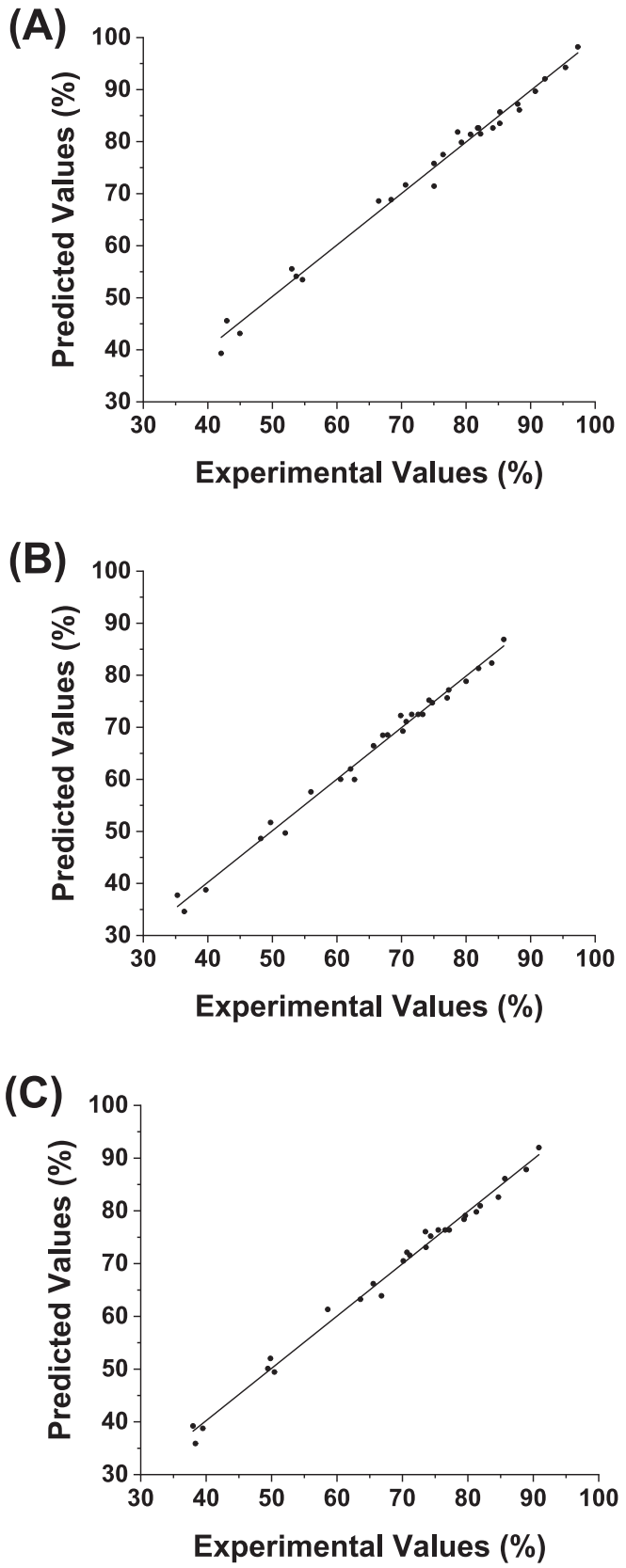

Fig. 6. Comparison plot between the experimental and model values predicted for the adsorption of TCS (%) using (A) Al-PILC$_{AE}$, (B) Al-PILC$_{BE}$, and (C) Al-PILC$_{CM}$.

(X_1X_3) and bed-depth was significant, as mentioned above in the "effect of pH" and "effect of adsorbent dose" sections. Finally, the two-way interaction with initial TCS concentration (X_3X_4) was significant for all three pillared clays tested.

3.3.4. *Effect of initial TCS concentration*

The initial pollutant concentration (10–30 mg/dm^3) was also studied. TCS adsorption was found to be very sensitive to changes in the initial concentration of pollutant used in the adsorption process. The initial concentration of adsorbate plays a significant role in the adsorption process by acting as an important driving force to overcome the mass-transfer resistance between the aqueous phase and the solid phase (Iqbal et al., 2016). The ratio between sorbent and sorbate is also relevant in the adsorption process, with a high ratio implying a lower sorbate concentration. TCS adsorption was found to be high at the lowest concentration using the three Al-PILC tested, which might be due to the higher ratio between sorbent and sorbate in these cases. When a lower number of molecules are present in the system, a higher surface area of adsorbent is available for each one to interact with, therefore the increase in interactions between both sorbent and sorbate favors the adsorption process. In contrast, when the ratio is lower, this indicates a higher concentration of pollutant, which results in saturation of the adsorption sites, thus causing aggregation and competition between the TCS molecules and, as a result, a decrease in the adsorption of the pollutant (Özer et al., 2009).

The effect of the initial concentration of TCS with respect to adsorbent dose (A), flux (B), and pH (C) for all three Al-PILCs studied as adsorbents is summarized in Figs. 7–9. Statistically, the effect of initial TCS concentration (X_4) and its pure quadratic interaction (X_4^2) were found to be strongly significant for all three pillared clays studied. The negative effect of both can be seen from Eqs. (19–21) and Fig. 5 for the three adsorbents studied. This clearly shows the inverse relationship between the initial TCS concentration and adsorption thereof. As was mentioned in the "*effect of pH*" and "*effect of sample flow rate*" sections above, the two-way interactions of initial TCS concentration with pH (X_1X_4) and flux (X_3X_4) were significant only for Al-PILC$_{BE}$ and for the three Al-PILCs, respectively.

3.4. *Solid-phase extraction*

The adsorption of TCS on the three adsorbents in fixed-bed systems was optimized to calculate the optimum conditions for the adsorption process. The values for the four independent variables for the adsorption of TCS in the fixed-bed system using the three different Al-PILCs as adsorbents are shown in Table 8. The highest adsorption of TCS using any of the three adsorbents was observed at an acidic pH (3.85–4.24), with the most acidic optimum value being obtained for Al-PILC$_{CM}$ (3.85), followed by Al-PILC$_{BE}$ (3.96) and Al-PILC$_{AE}$ (4.24). The optimum sample flow rate was the same for all three of them (0.5 cm^3/min), while the optimum concentration for the highest adsorption of TCS was close to the lowest value evaluated (1.13–2.56 mg/dm^3), with the lowest concentration being found for Al-PILC$_{CM}$ (1.13 mg/dm^3), followed by Al-PILC$_{BE}$ (1.93 mg/dm^3) and Al-PILC$_{AE}$ (2.56 mg/dm^3). The optimum amount of adsorbent was close to the highest value tested (367.78–378.93 mg), with the lowest value being found for Al-PILC$_{BE}$ (367.78 mg), followed by Al-PILC$_{AE}$ (378.04 mg) and Al-PILC$_{CM}$ (378.93 mg).

To evaluate the use of these Al-PILC as sorbents in SPE analysis, confirmatory experiments under the conditions found to be optimal for each adsorbent were performed in triplicate. Elution of TCS was complete in all three cases. Al-PILC$_{AE}$ showed complete adsorption of TCS under the optimized conditions, followed by Al-PILC$_{CM}$ (96.47 ± 0.85%) and Al-PILC$_{BE}$ (90.05 ± 2.97%). The highest relative error in the comparison between experimental and calculated adsorption values under these conditions was obtained for Al-PILC$_{BE}$ (1.89%). Our findings show that the models generated have satisfactory suitability and accuracy for

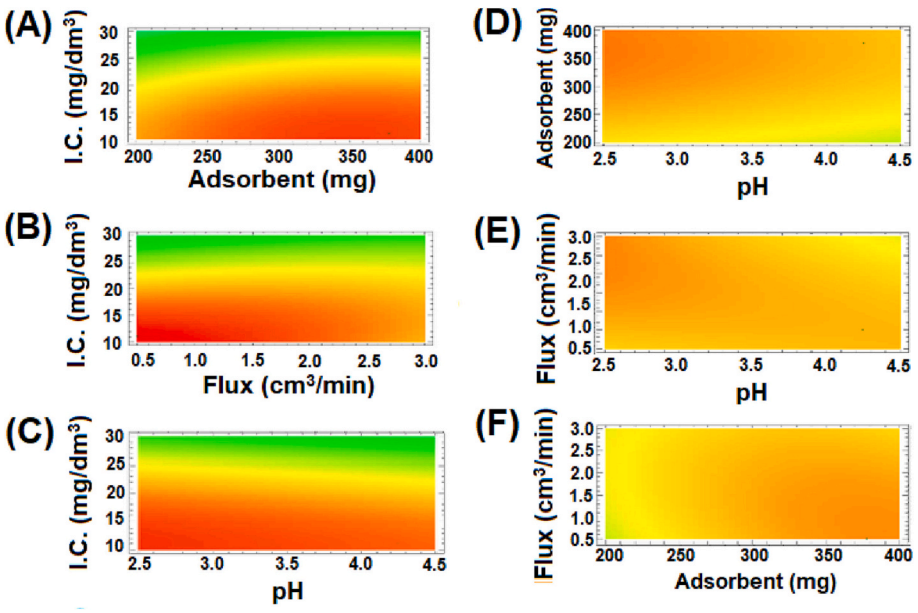

Fig. 7. 2D-response surface plots for the effect of (A) adsorbent and initial concentration, (B) flow rate and initial concentration, (C) pH and initial concentration, (D) pH and adsorbent, (E) pH and flow rate, and (F) adsorbent and flow rate, on TCS adsorption by Al-PILC$_{AE}$.

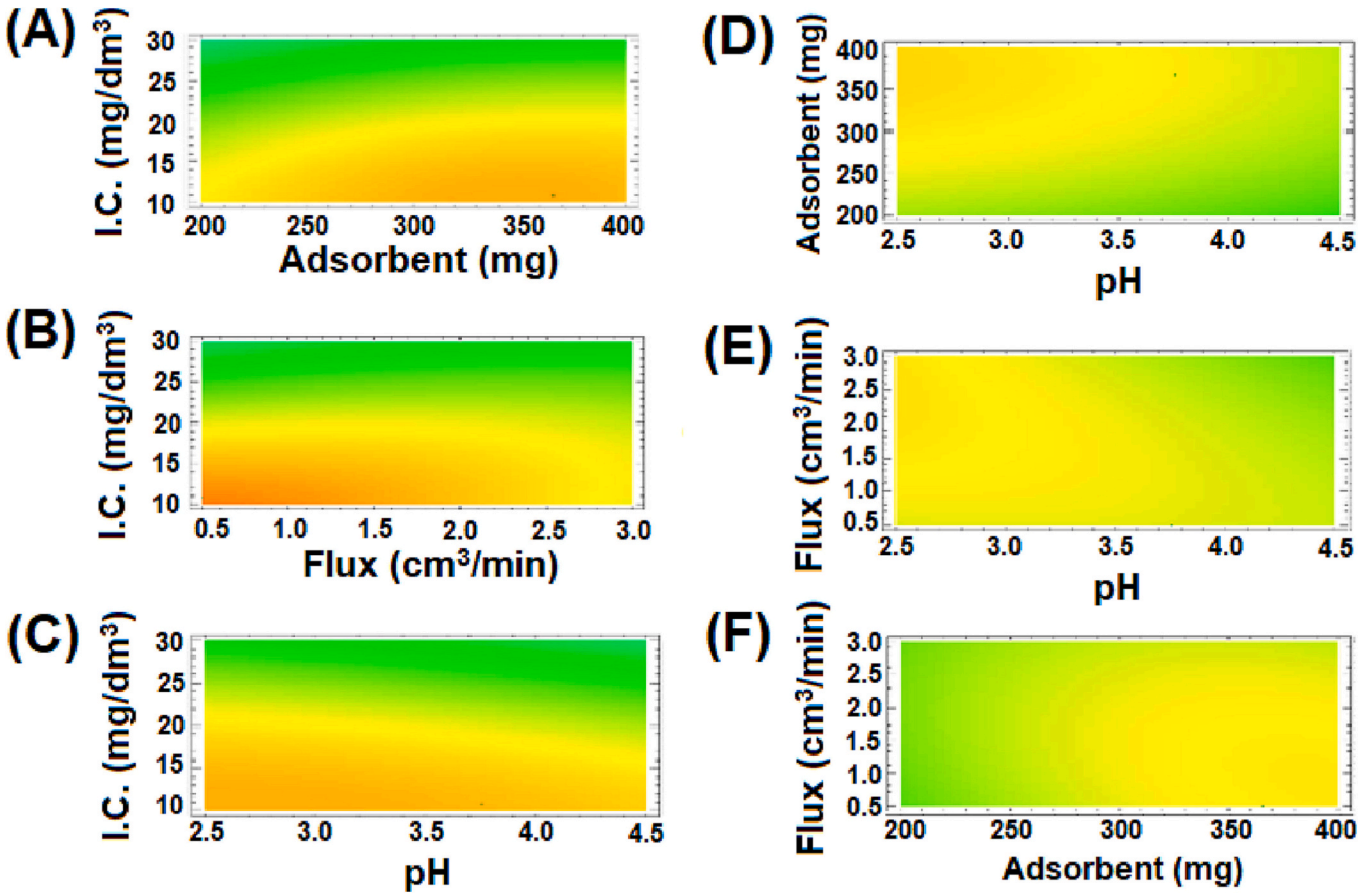

Fig. 8. 2D-response surface plots for the effect of (A) adsorbent and initial concentration, (B) flow rate and initial concentration, (C) pH and initial concentration, (D) pH and adsorbent, (E) pH and flow rate, and (F) adsorbent and flow rate, on TCS adsorption by Al-PILC$_{BE}$.

predicting the adsorption efficiency of TCS by the three Al-PILCs studied. In addition, the fact that the volume required to complete the elution of TCS is lower than the volume of the pollutant solution treated clearly indicates that Al-PILC could be considered to be candidates for use in SPE for the pre-concentration of pollutants in water samples for analytical purposes. In this study, the pre-concentration of TCS was between 1.3- and 1.5-times when using a spectrometer to quantify the TCS. The purpose of this study was to evaluate the potential use of these

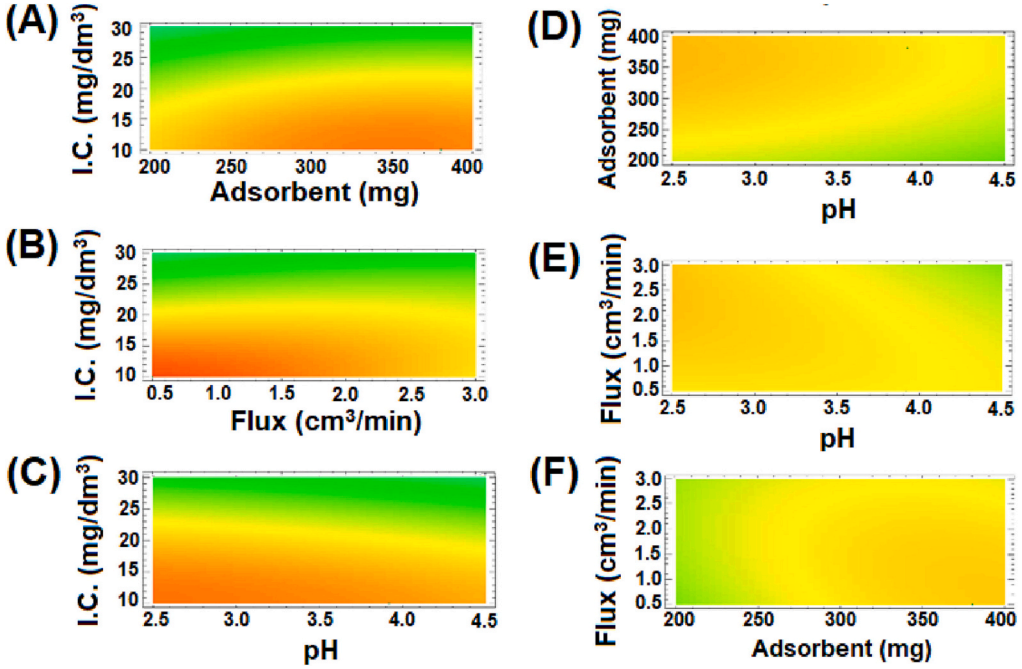

Fig. 9. 2D-response surface plots for the effect of (A) adsorbent and initial concentration, (B) flow rate and initial concentration, (C) pH and initial concentration, (D) pH and adsorbent, (E) pH and flow rate, and (F) adsorbent and flow rate, on TCS adsorption by Al-PILC$_{CM}$.

Table 8
Optimized parameters.

Variables	Optimum Values			
		Al-PILC$_{AE}$	Al-PILC$_{BE}$	Al-PILC$_{CM}$
x_1	pH	4.24	3.96	3.85
x_2	Adsorbent (mg)	378.04	367.78	378.93
x_3	Flux (cm^3/min)	0.50	0.50	0.50
x_4	TCS concentration (mg/dm^3)	2.56	1.93	1.13

synthetic Al-PILC in SPE by studying the optimum adsorption of TCS using RSM-BBD. Since the results indicated higher adsorption of TCS on the three Al-PILC at lower TCS inlet concentrations, the use of another quantification method, such as high performance liquid chromatography (HPLC), which has a lower limit of detection (LOD) and limit of quantitation (LOQ), may allow us to study the adsorption and elution at lower concentrations, possibly achieving higher pre-concentration values, thus making it extensible to EP, which are only permitted in water at ng/dm^3 concentrations. Both LOD and LOQ were determined in this study, using the method of the intercept and the average value of slope (Eqs. (22 and 23)), using 3.3 (LOD) and 10 (LOQ) as ratios, agree with the International Conference on Harmonization (ICH) guideline.

$$\mathrm{LOD} = 3.3\,\sigma/\mathrm{S} \tag{22}$$

$$\mathrm{LOQ} = 10\,\sigma/\mathrm{S} \tag{23}$$

where, σ is the standard deviation of the response and S corresponds to the slope of the calibration curve. Table S6 shows the parameters used as well as the LOD (0.1339 mg/dm^3) and LOQ (0.4058 mg/dm^3) calculated.

4. Summary and conclusions

This study has successfully developed a response surface methodology based on the Box–Behnken design (RSM-BBD) to optimize the adsorption of triclosan (TCS) by three alumina pillared clays (Al-PILC) in fixed-bed columns for use in solid phase extraction (SPE) analysis. Two of the Al-PILC were synthesized from an industrial waste known as saline slag, thus showing the environmentally friendly nature of this SPE method. Column performance was studied, and the breakthrough curves were investigated by varying process parameters such as the bed height (0.25–0.75 cm), inlet TCS concentration (20–60 mg/dm^3), and flow rate used (0.5–3 cm^3). Bohart-Adams, bed depth service time (BDST), and Thomas models were successfully applied to the fixed-bed results. For all three Al-PILC, higher breakthrough volumes were obtained with the use of high bed depths, low inlet flow rates, and low inlet concentrations. The adsorption conditions for TCS using an SPE cartridge as the column and the three Al-PILC as adsorbents were successfully optimized using RSM-BBD. The effects of four operating variables, namely bed heights of the adsorbents (0.25–1.0 cm), inlet TCS concentration (1–30 mg/dm^3), pH (2.5–4.5), and flow rate (0.5–3.0 mg/dm^3) on the adsorption of TCS (as response) were evaluated. The polynomial quadratic models developed agreed with the experimental data with 95% significance since high regression parameters were obtained (R^2 = 98.93–99.1), and the analysis of variance (ANOVA) confirmed the validity of the suggested models. Three-dimensional surface plots were generated to estimate the synergistic effects between the independent variables on adsorption efficiency. The results indicated that the inlet TCS concentration and bed height were the most significant independent variables affecting the adsorption of TCS in the fixed-bed column for all three Al-PILCs. Models were used to predict the optimum adsorption conditions, which were found to be 378.04, 367.78, and 378.93 mg (amount of adsorbent packed into the column), 0.5 cm^3/min (flow rate), 4.24, 3.96, and 3.85 (pH), and 2.56, 1.93, and 1.13 mg/dm^3 (inlet TCS concentration) for Al-PILC$_{AE}$, Al-PILC$_{BE}$, and Al-PILC$_{CM}$, respectively. The good agreement found between predicted values and those obtained from the confirmatory experiments (maximum of 1.89% relative error) confirmed the satisfactory suitability of the generated models to predict the adsorption of TCS on the Al-PILC packed into the SPE cartridges. Overall, these results corroborate that RSM-BDD is an effective and reliable tool for evaluating and optimizing the adsorption conditions for emerging contaminants in fixed-bed column systems. Al-PILC$_{AE}$ allowed complete adsorption of TCS under the optimized conditions, followed by Al-PILC$_{CM}$ (96.47 ± 0.85%) and Al-PILC$_{BE}$ (90.05 ± 2.97%). The elution of TCS was complete in all three cases. These results show that the three Al-

PILCs studied are good and promising adsorbents for TCS in the fixed-bed column used and that they can be used in the SPE system as adsorbents for analytical purposes. In addition, their use may be extended to the adsorption of other EP since the adsorbents investigated in this work have not been studied for the pre-concentration of other EP.

Funding

No funding was received for this work.

Research ethics

We further confirm that any aspect of the work covered in this manuscript that has involved human patients has been conducted with the ethical approval of all relevant bodies and that such approvals are acknowledged within the manuscript.

CRediT authorship contribution statement

Yaneth Cardona: Conceptualization, Formal analysis, Investigation, Methodology, Validation, Writing – original draft, Writing – review & editing. **Sophia A. Korili:** Funding acquisition, Supervision, Writing – review & editing. **Antonio Gil:** Conceptualization, Formal analysis, Funding acquisition, Methodology, Project administration, Resources, Supervision, Validation, Writing – original draft, Writing – review & editing.

Declaration of Competing Interest

None.

Data availability

No data was used for the research described in the article.

Acknowledgments

The authors are grateful for financial support from the Spanish Ministry of Science and Innovation (MCIN/AEI/10.13039/501100011033) through project PID2020-112656RB-C21. YC thanks the Universidad Pública de Navarra for a pre-doctoral grant (IberusTalent, European Union's H2020 research and innovation program under Marie Sklodowska-Curie grant agreement N° 801586). AG also thanks Banco Santander for funding via the Research Intensification Program.

Appendix A. Supplementary data

Supplementary data to this article can be found online at https://doi.org/10.1016/j.clay.2023.106879.

References

Abou-Taleb, K.A., Galal, G.F., 2018. A Comparative Study between One-Factor-at-a-Time and Minimum Runs Resolution-IV Methods for Enhancing the production of Polysaccharide by Stenotrophomonas Daejeonensis and Pseudomonas Geniculate. Ann. Agric. Sci. 63, 173–180. https://doi.org/10.1016/j.aoas.2018.11.002.

Allouss, D., Essamlali, Y., Amadine, O., Chakir, A., Zahouily, M., 2019. Response Surface Methodology for Optimization of Methylene Blue Adsorption onto Carboxymethyl Cellulose-based Hydrogel Beads: Adsorption Kinetics, Isotherm. Thermodyn. Reusabilit. Stud. RSC Adv. 9, 37858–37869. https://doi.org/10.1039/C9RA06450H.

Aly, A.A., Górecki, T., 2020. Green Approaches to Sample Preparation based on Extraction Techniques. Molecules 25. https://doi.org/10.3390/molecules25071719.

Ani, J.U., Okoro, U.C., Aneke, L.E., Onukwuli, O.D., Obi, I.O., Akpomie, K.G., Ofomatah, A.C., 2019. Application of Response Surface Methodology for Optimization of Dissolved Solids Adsorption by Activated Coal. Appl Water Sci 9, 60. https://doi.org/10.1007/s13201-019-0943-7.

Bohart, G.S., Adams, E.Q., 1920. Some Aspects of the Behavior of Charcoal with respect to Chlorine. J. Am. Chem. Soc. 42, 523–544. https://doi.org/10.1021/ja01448a018.

Cardona, Y., Korili, S.A., Gil, A., 2021. A Nonconventional Aluminum Source in the production of Alumina-Pillared Clays for the Removal of Organic Pollutants by Adsorption. Chem. Eng. J. 425, 130708 https://doi.org/10.1016/j.cej.2021.130708.

Cardona, Y., Vicente, M.A., Korili, S.A., Gil, A., 2022. Progress and Perspectives for the use of Pillared Clays as Adsorbents for Organic Compounds in Aqueous solution. Rev. Chem. Eng. 38 https://doi.org/10.1515/revce-2020-0015.

Dahane, S., Gil García, M.D., Uclés Moreno, A., Martínez Galera, M., del Socías Viciana, M.M., Derdour, A., 2015. Determination of eight Pesticides of varying Polarity in Surface Waters using Solid phase Extraction with Multiwalled Carbon Nanotubes and Liquid Chromatography-Linear Ion Trap Mass spectrometry. Microchim. Acta 182, 95–103. https://doi.org/10.1007/s00604-014-1290-x.

Demim, S., Drouiche, N., Aouabed, A., Benayad, T., Couderchet, M., Semsari, S., 2014. Study of Heavy Metal Removal from Heavy Metal Mixture using the CCD Method. J. Ind. Eng. Chem. 20, 512–520. https://doi.org/10.1016/j.jiec.2013.05.010.

Dubé, M.A., Salehpour, S., 2014. Applying the Principles of Green Chemistry to Polymer Production Technology. Macromol. React. Eng. 8, 7–28. https://doi.org/10.1002/mren.201300103.

Fu, Y., Pessagno, F., Manesiotis, P., Borrull, F., Fontanals, N., Maria Marcé, R., 2022. Preparation and Evaluation of Molecularly Imprinted Polymers as Selective SPE Sorbents for the Determination of Cathinones in River Water. Microchem. J. 175, 107100 https://doi.org/10.1016/j.microc.2021.107100.

Goel, J., Kadirvelu, K., Rajagopal, C., Kumar Garg, V., 2005. Removal of Lead(II) by Adsorption using Treated Granular Activated Carbon: batch and Column Studies. J. Hazard. Mater. 125, 211–220. https://doi.org/10.1016/j.jhazmat.2005.05.032.

Hennion, M.-C., Cau-Dit-Coumes, C., Pichon, V., 1998. Trace Analysis of Polar Organic Pollutants in Aqueous Samples: Tools for the Rapid Prediction and Optimisation of the Solid-phase Extraction Parameters. J. Chromatogr. A 823, 147–161. https://doi.org/10.1016/S0021-9673(98)00479-8.

Hutchins, R.A., 1973. New method simplifies design of activated carbon systems. Am. J. Chem. Eng. 80, 133–138.

Iqbal, M., Iqbal, N., Bhatti, I.A., Ahmad, N., Zahid, M., 2016. Response surface methodology application in optimization of cadmium adsorption by shoe waste: a good option of waste mitigation by waste. Ecol. Eng. 88, 265–275. https://doi.org/10.1016/j.ecoleng.2015.12.041.

Lee, V.K.C., Porter, J.F., McKay, G., 2000. Development of fixed-bed adsorber correlation models. Ind. Eng. Chem. Res. 39, 2427–2433. https://doi.org/10.1021/ie000017q.

López-Lorente, Á.I., Pena-Pereira, F., Pedersen-Bjergaard, S., Zuin, V.G., Ozkan, S.A., Psillakis, E., 2022. The ten principles of green sample preparation. TrAC Trends Anal. Chem. 148, 116530 https://doi.org/10.1016/j.trac.2022.116530.

Magro, C., Mateus, E.P., Paz-Garcia, J.M., Ribeiro, A.B., 2020. Emerging organic contaminants in wastewater: understanding electrochemical reactors for triclosan and its by-products degradation. Chemosphere 247, 125758. https://doi.org/10.1016/j.chemosphere.2019.125758.

Maiti, A., DasGupta, S., Basu, J.K., De, S., 2008. Batch and column study: adsorption of arsenate using untreated laterite as adsorbent. Ind. Eng. Chem. Res. 47, 1620–1629. https://doi.org/10.1021/ie070908z.

Maranata, G.J., Surya, N.O., Hasanah, A.N., 2021. Optimising factors affecting solid phase extraction performances of molecular imprinted polymer as recent sample preparation technique. Heliyon 7, e05934. https://doi.org/10.1016/j.heliyon.2021.e05934.

Mezcua, M., Gómez, M.J., Ferrer, I., Aguera, A., Hernando, M.D., Fernández-Alba, A.R., 2004. Evidence of 2,7/2,8-dibenzodichloro-p-dioxin as a Photodegradation product of Triclosan in Water and Wastewater Samples. Anal. Chim. Acta 524, 241–247. https://doi.org/10.1016/j.aca.2004.05.050.

Mourabet, M., El Rhilassi, A., El Boujaady, H., Bennani-Ziatni, M., Taitai, A., 2017. Use of response surface methodology for optimization of fluoride adsorption in an aqueous solution by brushite. Arab. J. Chem. 10, S3292–S3302. https://doi.org/10.1016/j.arabjc.2013.12.028.

Omidvar Borna, M., Pirsaheb, M., Vosoughi Niri, M., Khosravi Mashizie, R., Kakavandi, B., Zare, M.R., Asadi, A., 2016. Batch and column studies for the adsorption of Chromium(VI) on Low-cost Hibiscus Cannabinus Kenaf, a Green Adsorbent. J. Taiwan Inst. Chem. Eng. 68, 80–89. https://doi.org/10.1016/j.jtice.2016.09.022.

Özer, A., Gürbüz, G., Çalimli, A., Körbahti, B.K., 2009. Biosorption of copper(II) Ions on Enteromorpha Prolifera: application of response surface methodology (RSM). Chem. Eng. J. 146, 377–387. https://doi.org/10.1016/j.cej.2008.06.041.

Paíga, P., Delerue-Matos, C., 2013. Response surface methodology applied to SPE for the determination of Ibuprofen in various types of water samples. J. Sep. Sci. 36, 3220–3225. https://doi.org/10.1002/jssc.201300544.

Palencia, M., Lerma, T.A., Garcés, V., Mora, M.A., Martínez, J.M., Palencia, S.L., 2021. Chapter 21 - Removal of Emergent Pollutants of Waters. In: Palencia, M., Lerma, T. A., Garcés, V., Mora, M.A., Martínez, J.M., Palencia, S.L.B.T.-E.F.P. (Eds.), Advances in Green and Sustainable Chemistry. Elsevier, pp. 327–340. https://doi.org/10.1016/B978-0-12-821842-6.00023-3.

Patel, H., 2020. Batch and Continuous Fixed Bed Adsorption of Heavy Metals Removal using Activated Charcoal from Neem (Azadirachta Indica) Leaf Powder. Sci. Rep. 10, 16895. https://doi.org/10.1038/s41598-020-72583-6.

Poole, C.F., 2003. New Trends in Solid-phase Extraction. TrAC Trends Anal. Chem. 22, 362–373. https://doi.org/10.1016/S0165-9936(03)00605-8.

Raccary, B., Loubet, P., Peres, C., Sonnemann, G., 2022. Life cycle assessment of sample preparation in analytical chemistry: a case study on SBSE and SPE Techniques. Adv. Sample Prep. 1, 100009 https://doi.org/10.1016/j.sampre.2022.100009.

Samarghandi, M.R., Hadi, M., McKay, G., 2014. Breakthrough curve analysis for fixed-bed adsorption of azo dyes using novel pine cone—derived active carbon. Adsorpt. Sci. Technol. 32, 791–806. https://doi.org/10.1260/0263-6174.32.10.791.

Sanchez-Prado, L., Llompart, M., Lores, M., García-Jares, C., Bayona, J.M., Cela, R., 2006. Monitoring the photochemical degradation of Triclosan in Wastewater by UV Light and Sunlight using Solid-phase Microextraction. Chemosphere 65, 1338–1347. https://doi.org/10.1016/j.chemosphere.2006.04.025.

Shojaei, Siroos, Shojaei, Saeed, Band, S.S., Farizhandi, A.A.K., Ghoroqi, M., Mosavi, A., 2021. Application of Taguchi method and response surface methodology into the removal of malachite green and Auramine-O by NaX Nanozeolites. Sci. Rep. 11, 16054. https://doi.org/10.1038/s41598-021-95649-5.

Tan, I.A.W., Ahmad, A.L., Hameed, B.H., 2009. Adsorption isotherms, kinetics, thermodynamics and desorption studies of 2,4,6-trichlorophenol on oil palm empty Fruit bunch-based activated carbon. J. Hazard. Mater. 164, 473–482. https://doi.org/10.1016/j.jhazmat.2008.08.025.

Tenkov, K.S., Dubinin, M.V., Vedernikov, A.A., Chelyadnikova, Y.A., Belosludtsev, K.N., 2022. An in vivo study of the toxic effects of triclosan on Xenopus laevis (Daudin, 1802) frog: Assessment of viability, tissue damage and mitochondrial dysfunction. Comp. Biochem. Physiol. Part C Toxicol. Pharmacol. 259, 109401 https://doi.org/10.1016/j.cbpc.2022.109401.

Thomas, H.C., 1944. Heterogeneous Ion Exchange in a Flowing System. J. Am. Chem. Soc. 66, 1664–1666. https://doi.org/10.1021/ja01238a017.

Tohidi, F., Cai, Z., 2017. Fate and mass balance of triclosan and its degradation products: comparison of three different types of wastewater treatments and aerobic/anaerobic sludge digestion. J. Hazard. Mater. 323, 329–340. https://doi.org/10.1016/j.jhazmat.2016.04.034.

Toor, M., Jin, B., 2012. Adsorption characteristics, isotherm, kinetics, and diffusion of modified natural bentonite for removing diazo dye. Chem. Eng. J. 187, 79–88. https://doi.org/10.1016/j.cej.2012.01.089.

Vijayaraghavan, K., Jegan, J., Palanivelu, K., Velan, M., 2004. Removal of Nickel(II) Ions from Aqueous solution using Crab Shell Particles in a Packed Bed Up-Flow Column. J. Hazard. Mater. 113, 223–230. https://doi.org/10.1016/j.jhazmat.2004.06.014.

Walker, G.M., Weatherley, L.R., 1997. Adsorption of acid dyes on to granular activated carbon in fixed beds. Water Res. 31, 2093–2101. https://doi.org/10.1016/S0043-1354(97)00039-0.

Wang, Y., Liang, W., 2021. Occurrence, Toxicity, and removal methods of triclosan: a timely review. Curr. Pollut. Rep. 7, 31–39. https://doi.org/10.1007/s40726-021-00173-9.

Wang, S., Chen, Z., Wang, Z., Fu, Y., Liu, Y., 2021. Enhanced degradation of Triclosan using UV–Fe2+ Synergistic activation of peracetic acid. Environ. Sci. Water Res. Technol. 7, 630–637. https://doi.org/10.1039/D0EW01095B.

Zheng, Y., Wang, A., 2010. Removal of Heavy Metals using polyvinyl Alcohol Semi-IPN Poly(acrylic acid)/tourmaline Composite Optimized with Response Surface Methodology. Chem. Eng. J. 162, 186–193. https://doi.org/10.1016/j.cej.2010.05.027.